



**The Abdus Salam
International Centre for Theoretical Physics**



2031-3

**Joint ICTP/IAEA School on Novel Synchrotron Radiation
Applications**

16 - 20 March 2009

Beamlines and Beam Optics

Anna Bianco
*Sincrotrone Trieste
Italy*



The Abdus Salam
International Centre for Theoretical Physics



Beamlines and Beam Optics

Anna Bianco

SINCROTRONE TRIESTE, ITALY

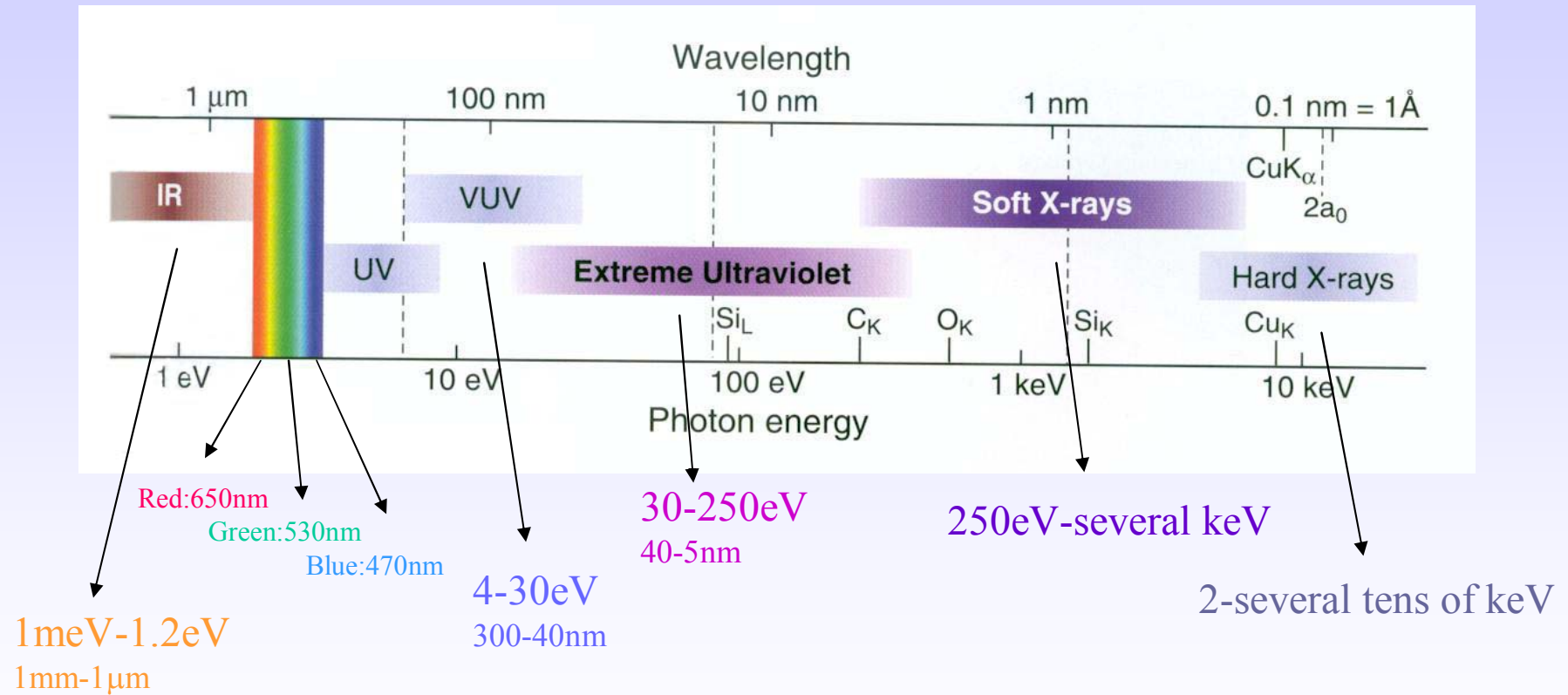
*Joint ICTP/IAEA School on Novel Synchrotron Radiation
Applications, Trieste, Italy, 16-20 March 2009*

Main properties of Synchrotron Radiation

- Very broad and continuous spectral range, from infrared up to soft and hard x-rays
- High intensity
- Highly collimated and emanates from a very small source: the electron beam
- Pulse time structure
- High degree of polarization

Spectral range

$$E(eV) = \frac{1240}{\lambda(nm)}$$



D.Attwood, "Soft x-rays and extreme ultraviolet radiation", Cambridge University Press, 1999

Main properties of Synchrotron Radiation

- Very broad and continuous spectral range, from infrared up to soft and hard x-rays
- High intensity
- Highly collimated and emanates from a very small source: the electron beam
- Pulse time structure
- High degree of polarization

Spectral brightness

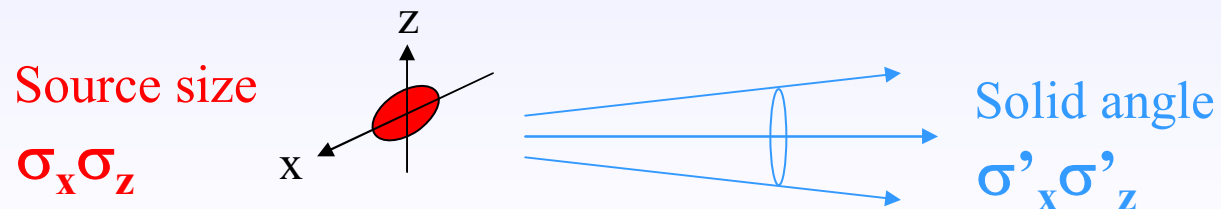
$$\text{Spectral Brightness} = \frac{\text{photon flux}}{I} \frac{1}{\sigma_x \sigma_z \sigma'_x \sigma'_z BW}$$

I = electron current in the storage ring, usually 100mA

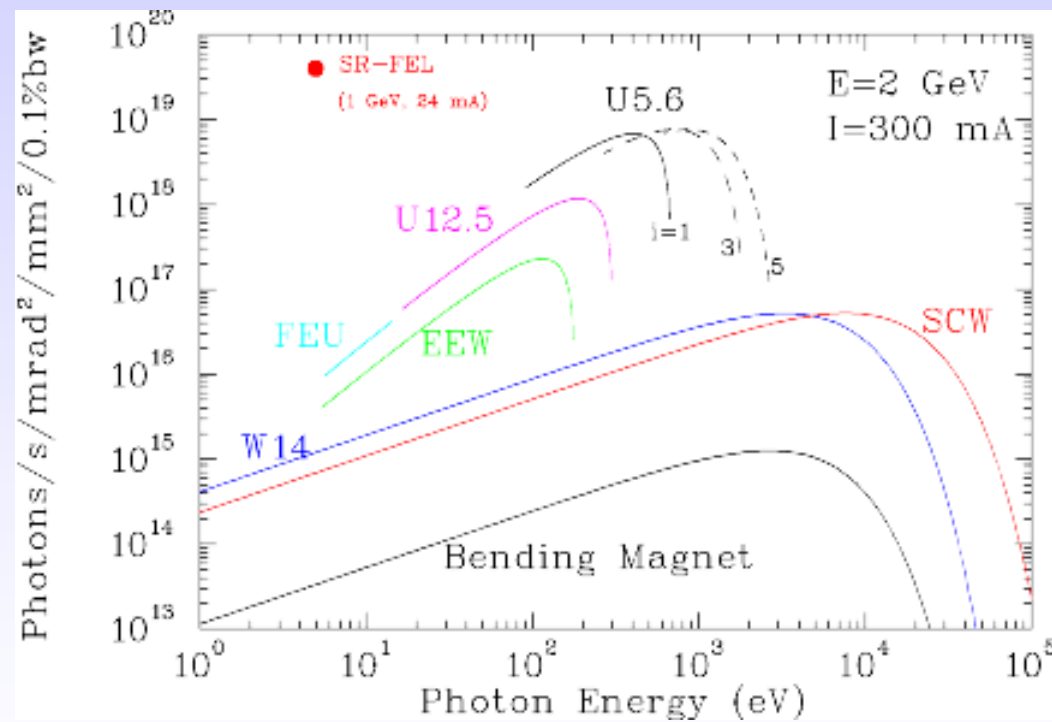
$\sigma_x \sigma_z$ = transverse area from which SR is emitted

$\sigma'_x \sigma'_z$ = solid angle into which SR is emitted

BW = spectral bandwidth, usually: $\frac{\Delta E}{E} = 0.1\%$



SR spectral brightness at ELETTRA



Why is brightness important? (1)

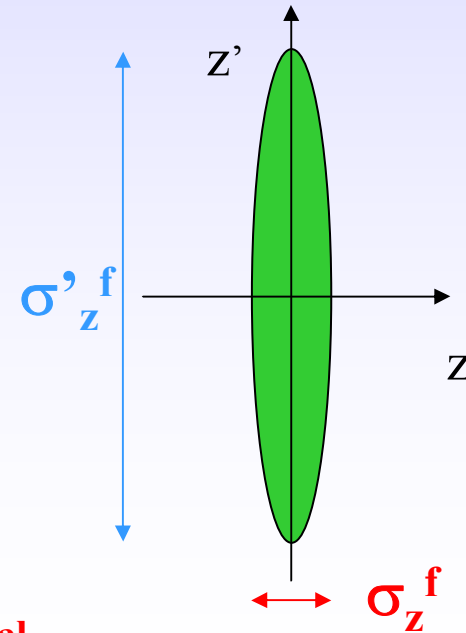
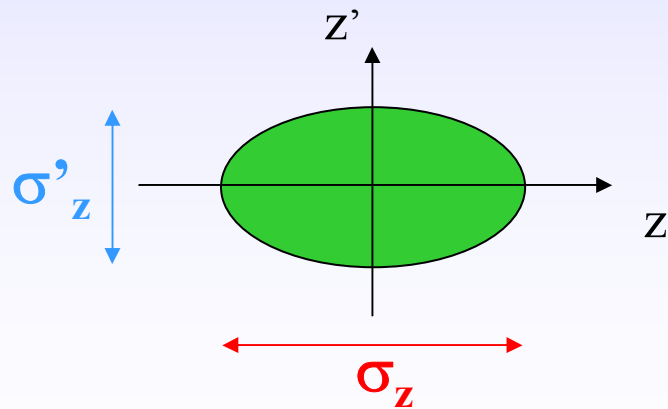
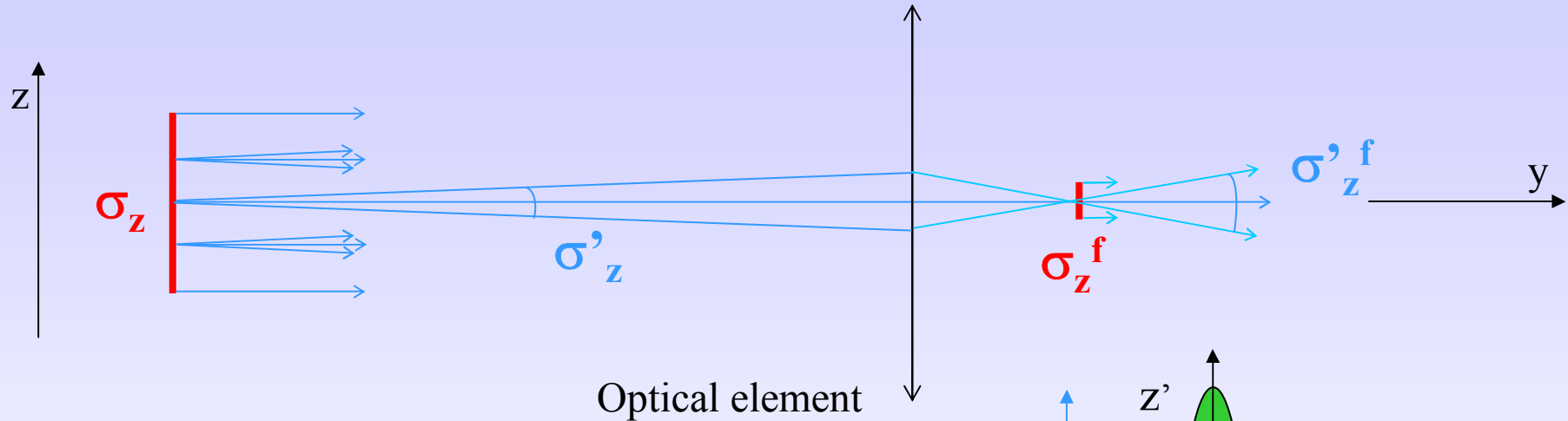
$$\text{Spectral Brightness} = \frac{\text{photon flux}}{I} \frac{1}{\sigma_x \sigma_z \sigma'_x \sigma'_z BW}$$

More flux \rightarrow more signal at the experiment

But why combining the flux with geometrical factors?

Liouville's theorem: for an optical system the occupied phase space volume cannot be decreased along the optical path (without losing photons) $\rightarrow (\sigma\sigma')_{\text{final}} \geq (\sigma\sigma')_{\text{initial}}$

Example : a focusing beam



Liouville's theorem: $(\sigma\sigma')_{\text{final}} \geq (\sigma\sigma')_{\text{initial}}$

Why is brightness important? (2)

To focus the beam in a small spot (which is needed for achieving energy and/or spatial resolution) one must accept an increase in the beam divergence.

Not bright source:
 $(\sigma\sigma')_{\text{initial}}$ large

+

Liouville's theorem:
 $(\sigma\sigma')_{\text{final}} \geq (\sigma\sigma')_{\text{initial}}$

→ high beam divergence

High beam divergence along the beamline:

- high optical aberrations
- large optical devices
- high costs and low optical qualities

With a not bright source the spot size can be made small only reducing the photon flux.

The high spectral brightness of the radiation source allows the development of monochromators with high energy resolution and high throughput and gives also the possibility to image a beam down to a very small spot on the sample with high intensity.

The beamline (1)

The researcher needs at his experiment a certain number of photons/second into a phase volume of some particular characteristics. Moreover, these photons have to be monochromatized.

The beamline:

- *is the means of bringing radiation from the source to the experiment transforming the phase volume in a controlled way: it de-magnifies, monochromatizes and refocuses the source onto a sample*
- *must preserve the excellent qualities of the radiation source: it must transfer the high brightness from source up to the experiment*

Conserving brightness

Brightness decreases because of:

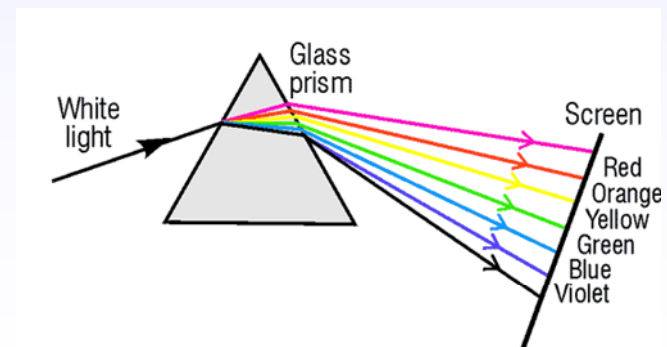
- micro-roughness and slope errors on optical surfaces
- thermal deformations of optical elements due to heat load produced by the high power radiation
- aberrations of optical elements

The beamline (2)

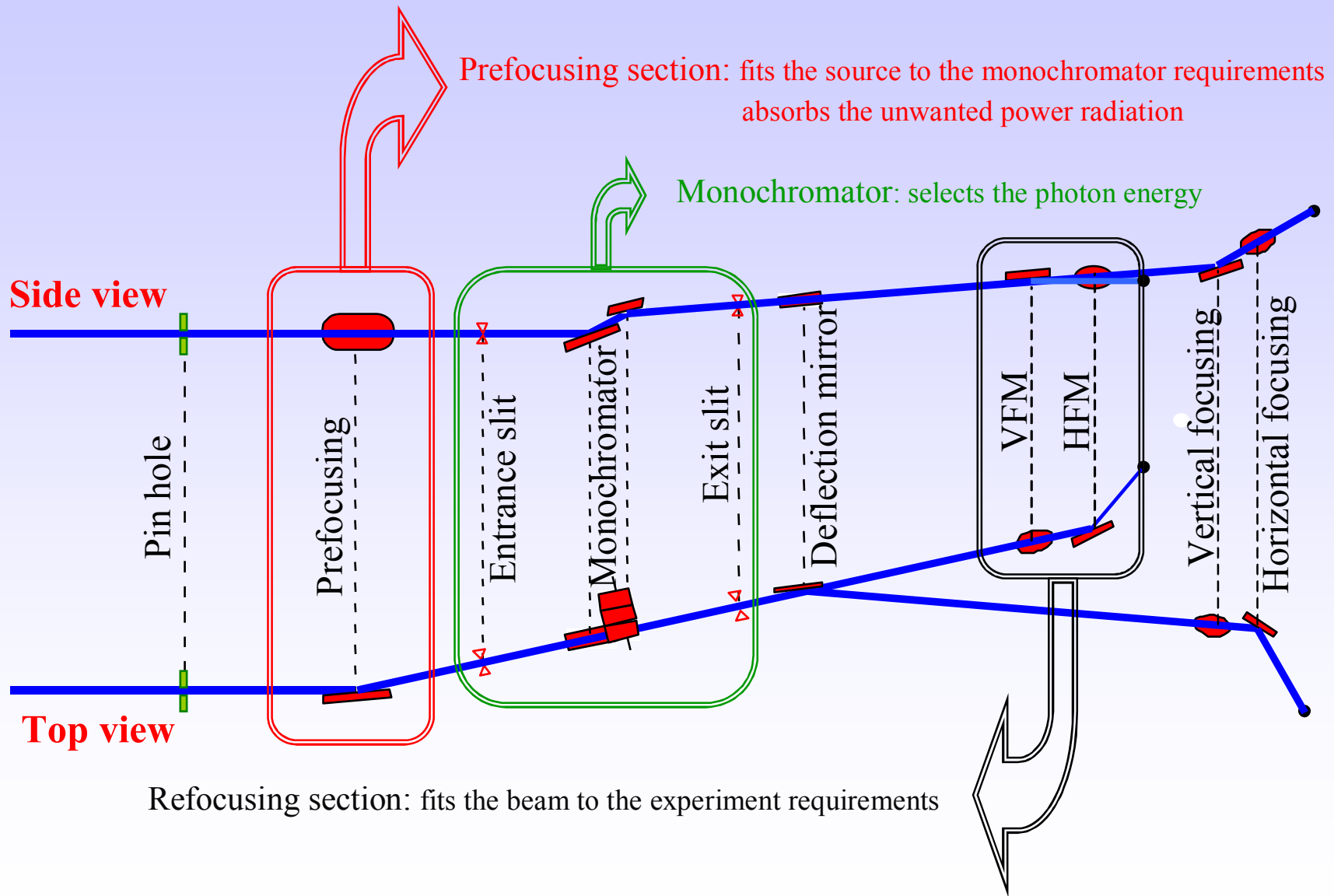
Not a simple pipe!

Basic optical elements:

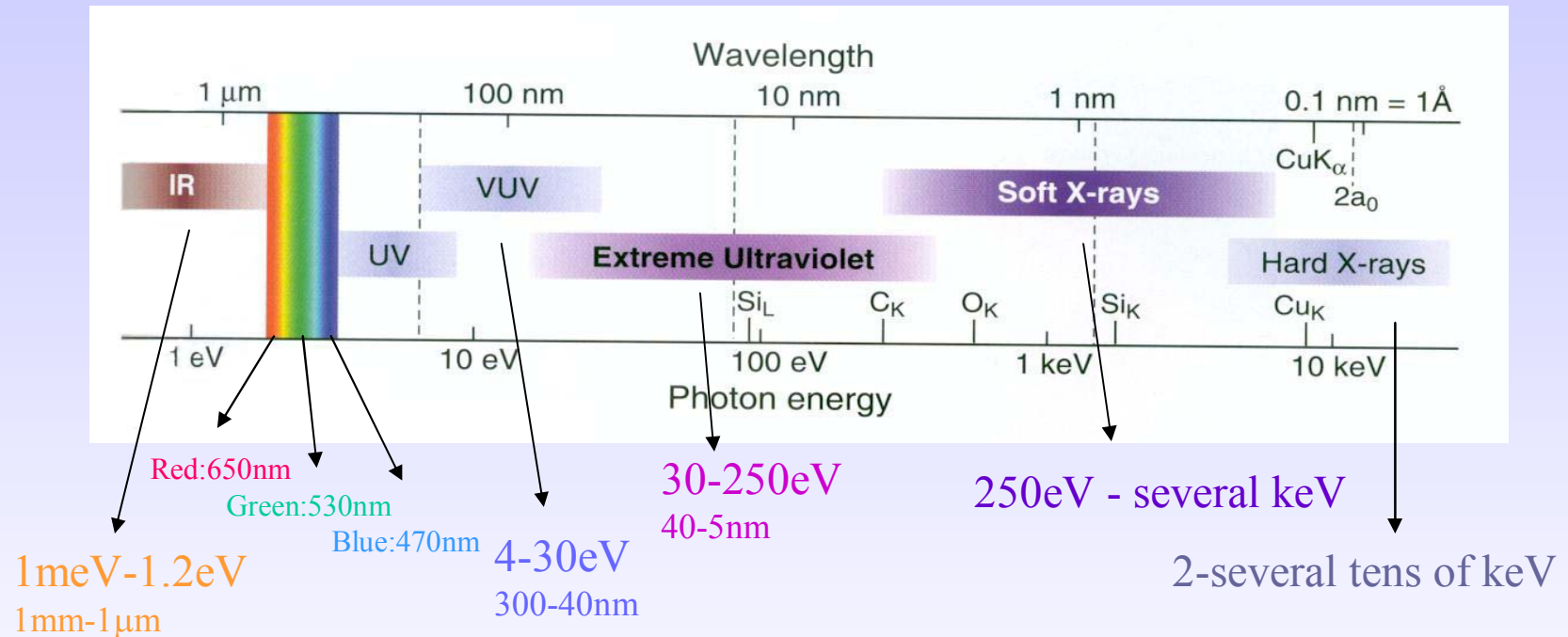
- mirrors, to deflect, focus and filter the radiation
- monochromators (gratings and crystals), to select photon energy



Beamline structure



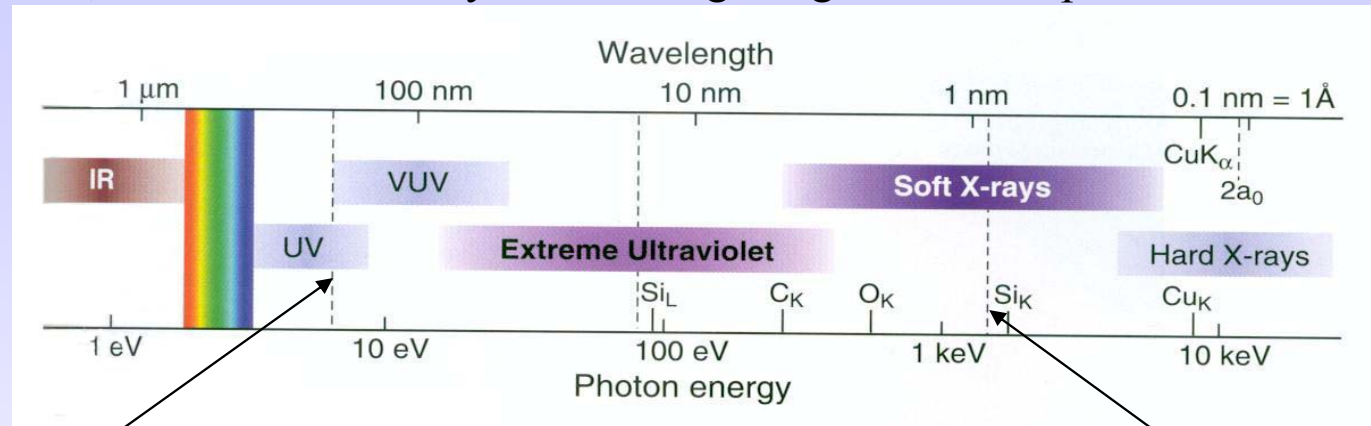
VUV, EUV and soft x-rays



These regions are very interesting because they are characterized by the presence of the absorption edges of most low and intermediate Z elements
→ photons with these energies are a **very sensitive tool** for elemental and chemical identification
But... these regions are difficult to access.

Ultra-high vacuum

VUV, EUV and soft x-rays have a high degree of absorption in all materials:



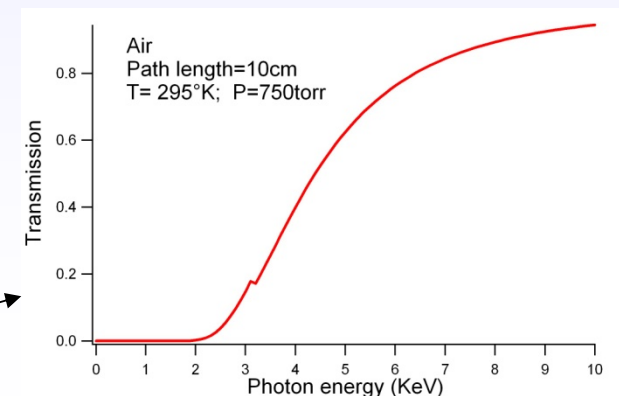
Transmission limit of common fused silica window: ~8eV Absorption limit of 8μm Be foil: ~1.5keV

- No windows
- The entire optical system must be kept under UH Vacuum

Ultrahigh vacuum conditions ($P=1-2 \times 10^{-9}$ mbar) are required:

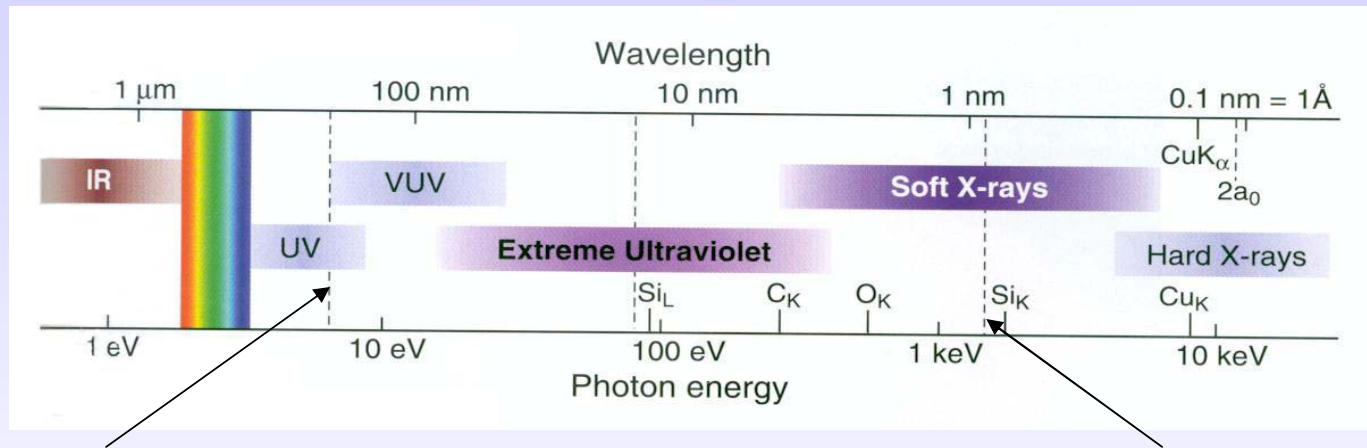
- Not to disturb the storage ring and the experiment
- To avoid photon absorption in air
- To protect optical surfaces from contamination (especially from carbon)

In the hard x-ray region, it is not necessary to use UHV:



No refractive optics

VUV, EUV and soft x-rays have a high degree of absorption in all materials:

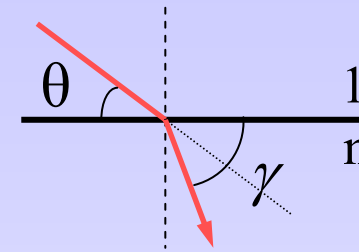


Transmission limit of common fused silica window: $\sim 8\text{eV}$ Absorption limit of $8\mu\text{m}$ Be foil: $\sim 1.5\text{keV}$

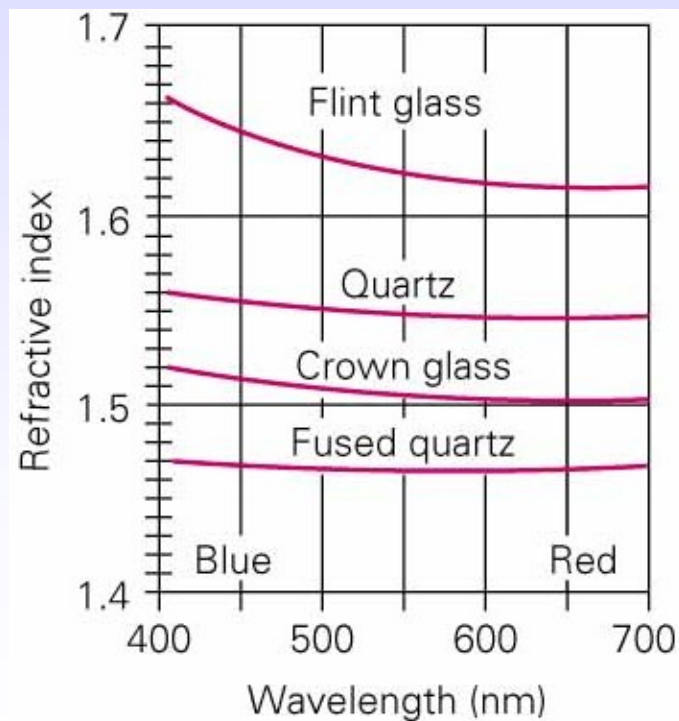
- The only optical elements which can work in the VUV, EUV and soft x-rays regions are mirrors and diffraction gratings, used in total external reflection at grazing incidence angles

Snell's law, visible light

$$n_1 \cos \theta = n_2 \cos \gamma$$
$$\rightarrow \cos \theta = n \cos \gamma \quad \text{with } n = n_2/n_1$$



$$n > 1 \rightarrow \gamma > \theta$$



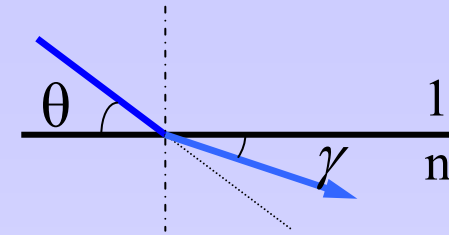
Visible light, when entering a medium of greater refractive index, is bent towards the surface normal.

This is the case for visible light impinging from air on a glass

Snell's law, X-rays

$$n_1 \cos \theta = n_2 \cos \gamma$$

$$\rightarrow \cos \theta = n \cos \gamma \quad \text{with } n = n_2/n_1$$



$$n < 1 \rightarrow \gamma < \theta$$

X-rays have the real part, n , of the **refractive index** slightly less than unity:

$$n = 1 - \delta \quad \text{where the } 0 < \delta \ll 1$$

Typical values are:

$$\delta \approx 10^{-2} \text{ for } 250\text{eV (5nm)}$$

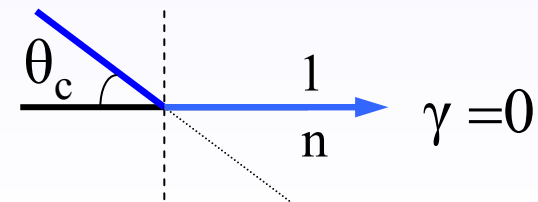
$$\delta \approx 10^{-4} \text{ for } 2.5\text{keV (0.5nm)}$$

→ X-ray radiation is refracted in a direction slightly further from the surface normal

→ the refraction angle γ can equal 0, indicating that the refracted wave doesn't penetrate into the material but rather propagates along the interface.

The limiting condition occurs at the **critical angle of incidence** θ_c : $\cos \theta_c = n$

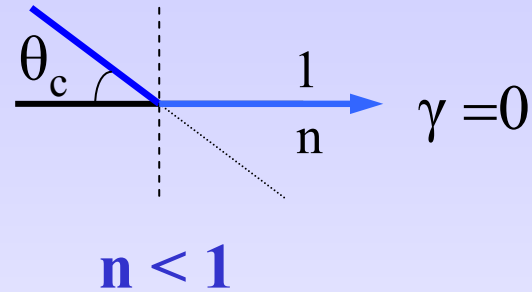
$$\rightarrow \boxed{\theta_c = \sqrt{2\delta}}$$



$$n < 1$$

Critical angle

$$\theta_c = \sqrt{2\delta}$$



Substituting δ , it can be shown that the major functional dependencies of θ_c are:

$$\theta_c \propto \lambda \sqrt{Z}$$

θ_c increases working at lower photon energy and using a material of higher atomic number Z .

Gold:

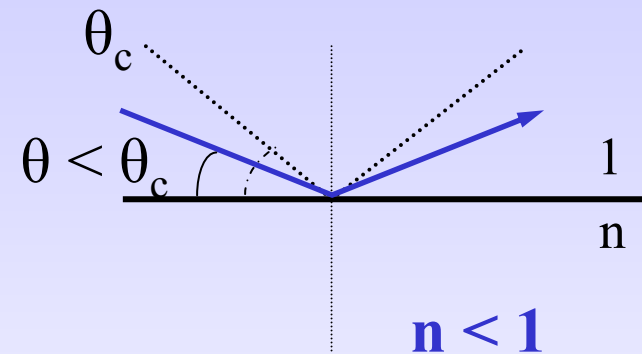
$$600 \text{ eV} \rightarrow \theta_c \approx 7.4^\circ$$

$$1200 \text{ eV} \rightarrow \theta_c \approx 3.7^\circ$$

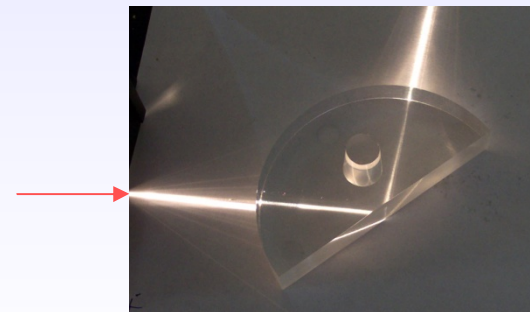
$$5 \text{ keV} \rightarrow \theta_c \approx 0.9^\circ$$

Total external reflection

If radiation impinges at a grazing angle $\theta < \theta_c$, it is **totally external reflected**.



It is the counterpart of total internal reflection of visible light. Visible light is totally reflected at the glass/air boundary if $\theta < \theta_c = 48.2^\circ$



$$n \cdot \cos \theta_c = 1 \rightarrow \theta_c = \arccos(1/n) = 48.2^\circ$$

$n = 1.5$ refraction index of glass

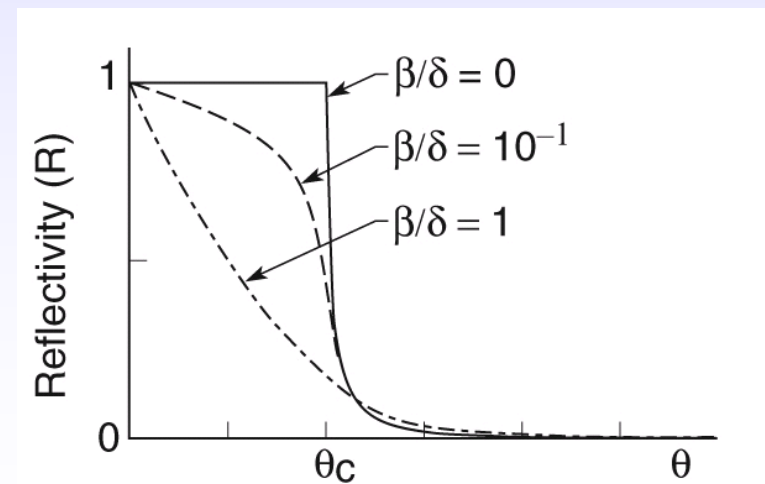
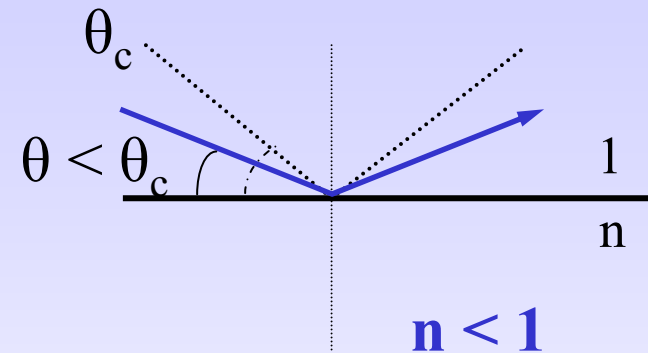
Nearly total external reflection

This model of total reflection is incomplete because it doesn't include the effect of the imaginary part of the refractive index.

$$\text{refractive index} = 1 - \delta + i\beta$$

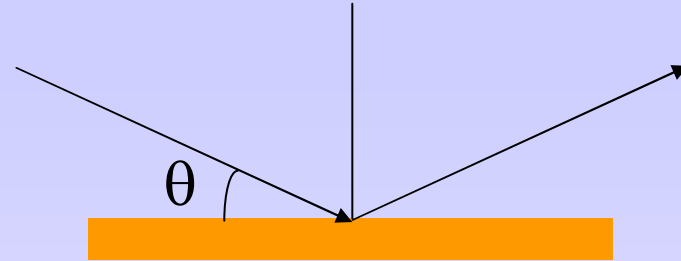
The radiation penetrates into the second medium during the reflection process, so that the absorption in this medium decreases the intensity of the reflected beam.

→ The sharpness of the cut-off is reduced

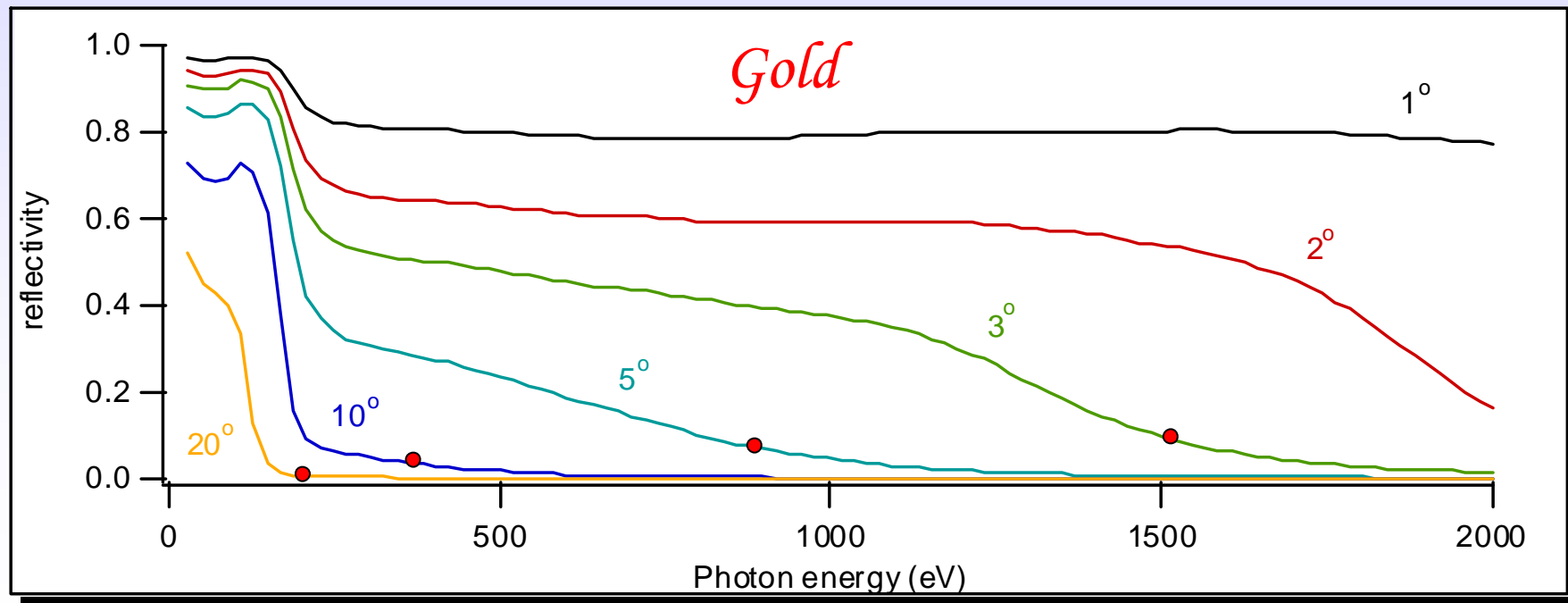


D.Attwood, "Soft x-rays and extreme ultraviolet radiation", Cambridge University Press, 1999

Mirror reflectivity (1)

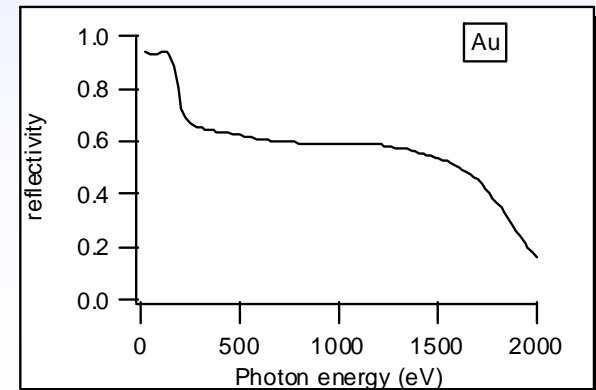
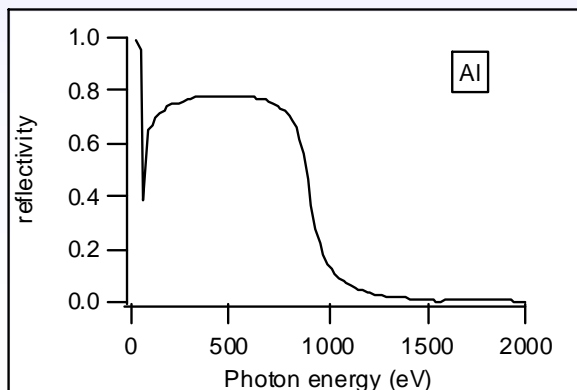
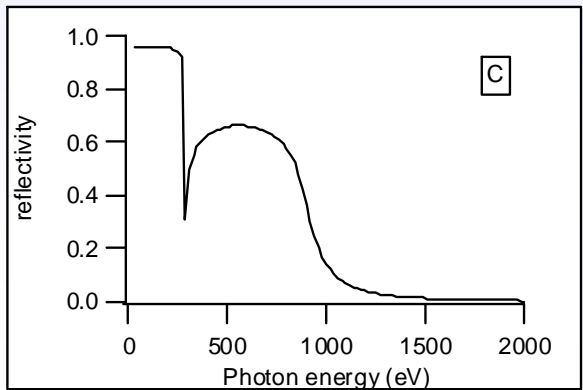
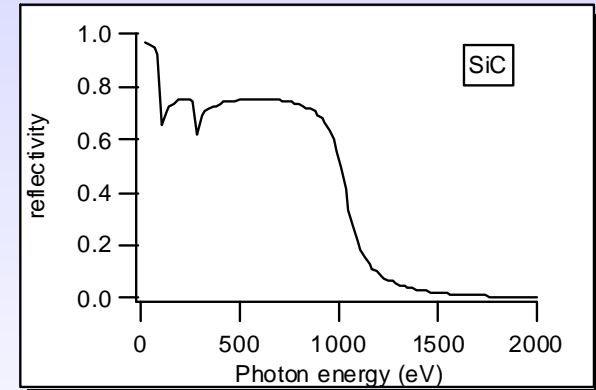
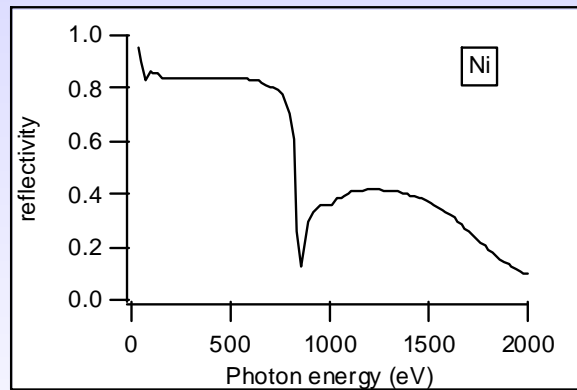
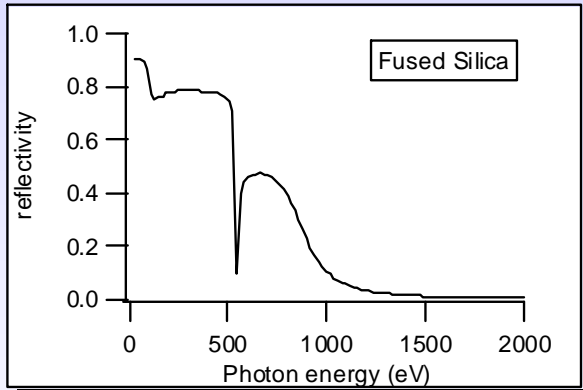
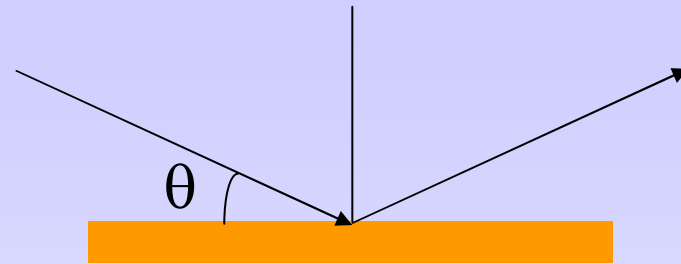


Reflectivity drops down fast with the increasing of the grazing incidence angle
→ only reflective optics at grazing incidence angles
(typically 1° - 2° for soft x-rays, few mrad for hard x-rays, $1 \text{ mrad} = 0.057^\circ$)



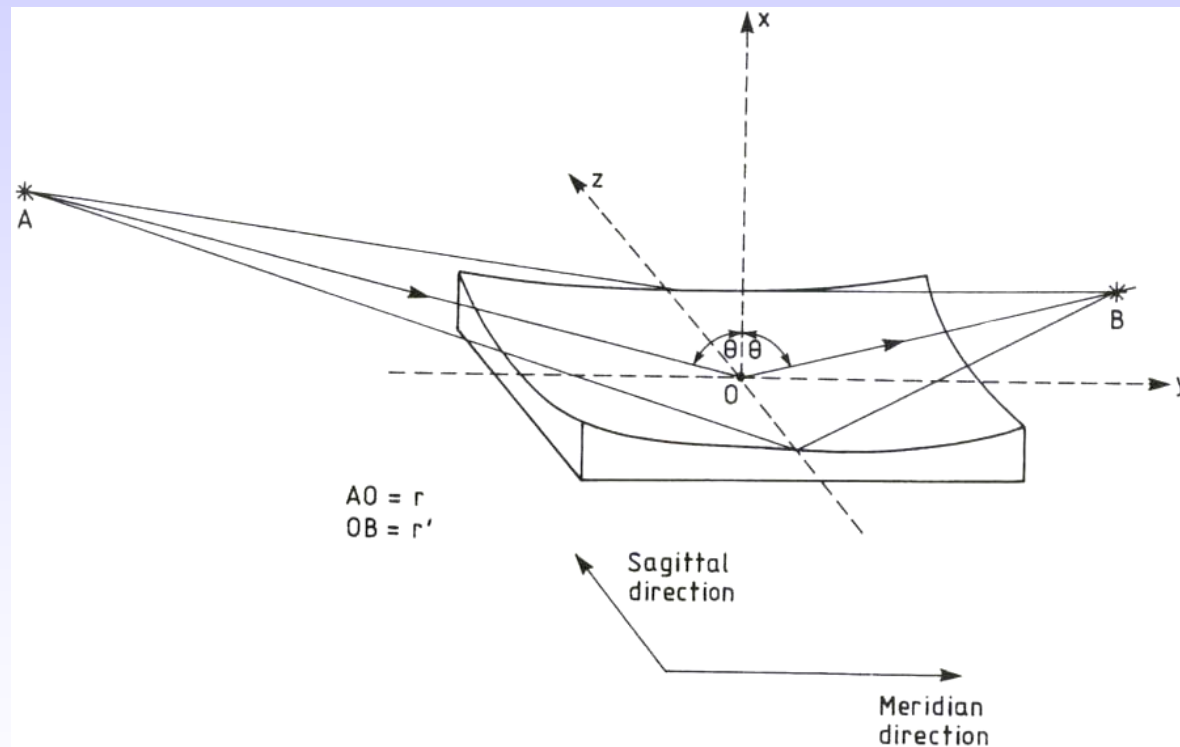
Mirror reflectivity (2)

$$\theta = 2^\circ$$



Focusing properties of mirrors

X-rays mirrors can have different geometrical shapes, their optical surface can be a plane, a sphere, a paraboloid, an ellipsoid and a toroid.



The **meridional** or **tangential plane** contains the central incident ray and the normal to the surface. The **sagittal plane** is the plane perpendicular to the tangential plane and containing the normal to the surface.

Paraboloid

Rays traveling parallel to the symmetry axis OX are all focused to a point A.

Conversely, the parabola collimates rays emanating from the focus A.

Line equation: $Y^2 = 4aX$

Paraboloid equation: $Y^2 + Z^2 = 4aX$

where: $a = f \cos^2 \vartheta$

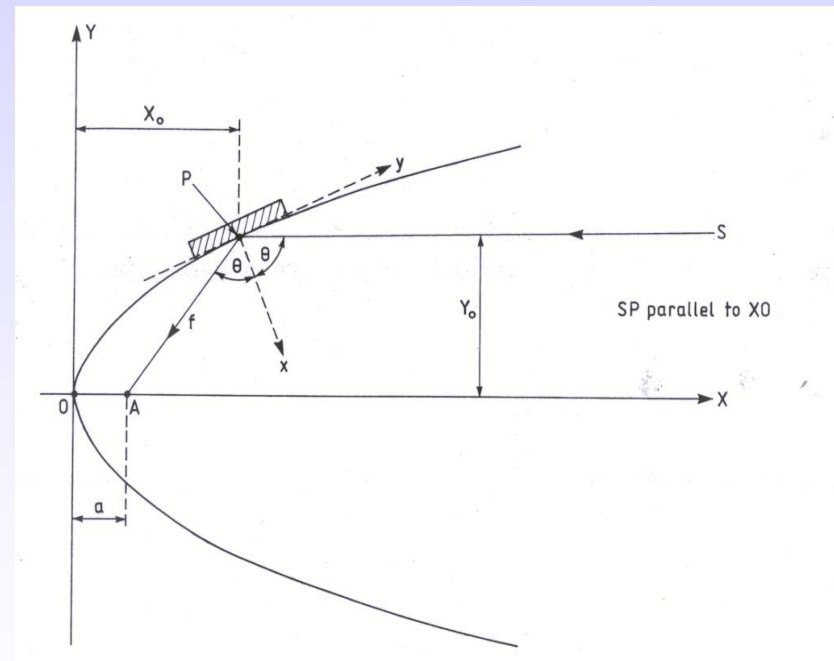
Position of the pole P:

$$X_o = a \tan^2 \vartheta$$

$$Y_o = 2a \tan \vartheta$$

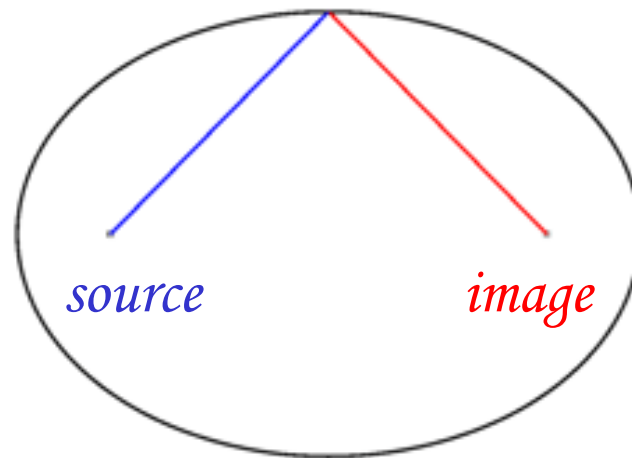
Paraboloid equation:

$$x^2 \sin^2 \vartheta + y^2 \cos^2 \vartheta + z^2 - 2xy \sin \vartheta \cos \vartheta - 4ax \sec \vartheta = 0$$



Ellipse

The ellipse has the property that rays from one point focus F_1 will always be perfectly focused to the second point focus F_2



Ellipsoid

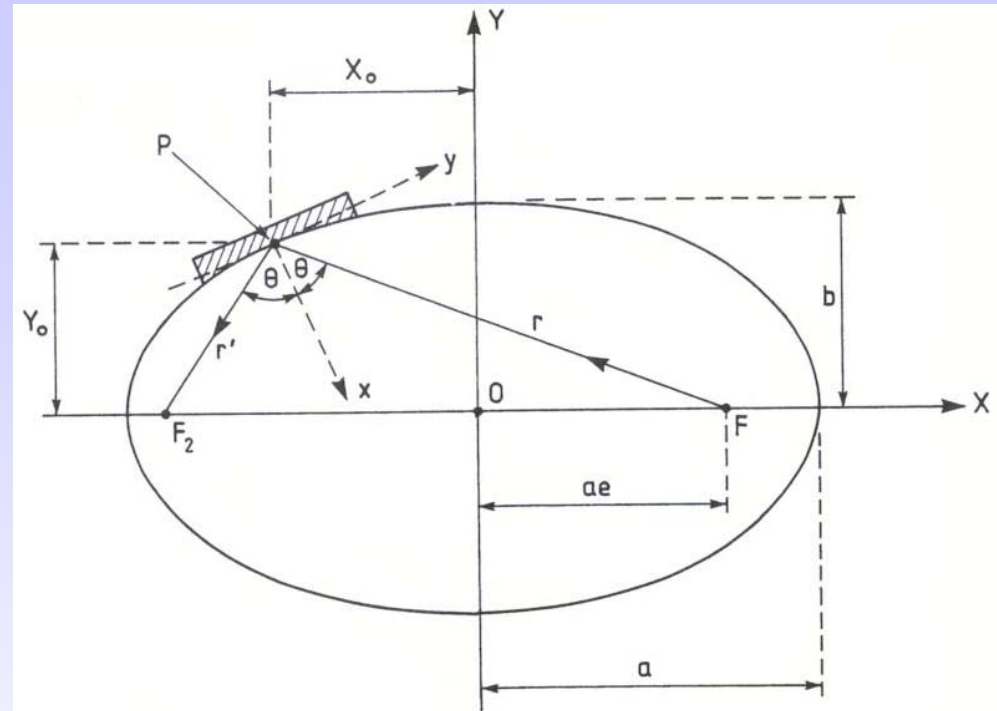
Line equation: $\frac{X^2}{a^2} + \frac{Y^2}{b^2} = 1$

Ellipsoid equation:

$$\frac{X^2}{a^2} + \frac{Y^2}{b^2} + \frac{Z^2}{b^2} = 1$$

where: $a = \frac{r + r'}{2}$; $b = a\sqrt{1 - e^2}$

$$e = \frac{1}{2a} \sqrt{r^2 + r'^2 - 2rr' \cos(2\vartheta)}$$



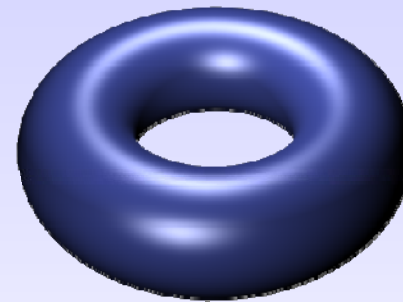
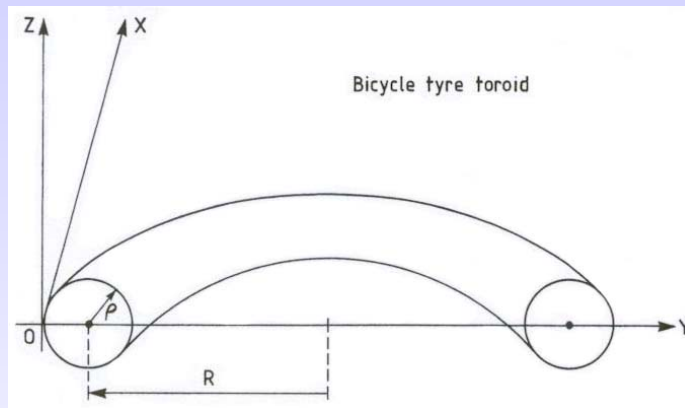
Rays from one focus F_1 will always be perfectly focused to the second focus F_2 .

$$x^2 \left(\frac{\sin^2 \vartheta}{b^2} + \frac{1}{a^2} \right) + y^2 \left(\frac{\cos^2 \vartheta}{b^2} \right) + \frac{z^2}{b^2} - x \left(\frac{4f \cos \vartheta}{b^2} \right) - xy \left[\frac{2 \sin \vartheta \sqrt{e^2 - \sin^2 \vartheta}}{b^2} \right] = 0$$

where: $f = \left(\frac{1}{r} + \frac{1}{r'} \right)^{-1}$

J.B. West and H.A. Padmore, Optical Engineering, 1987

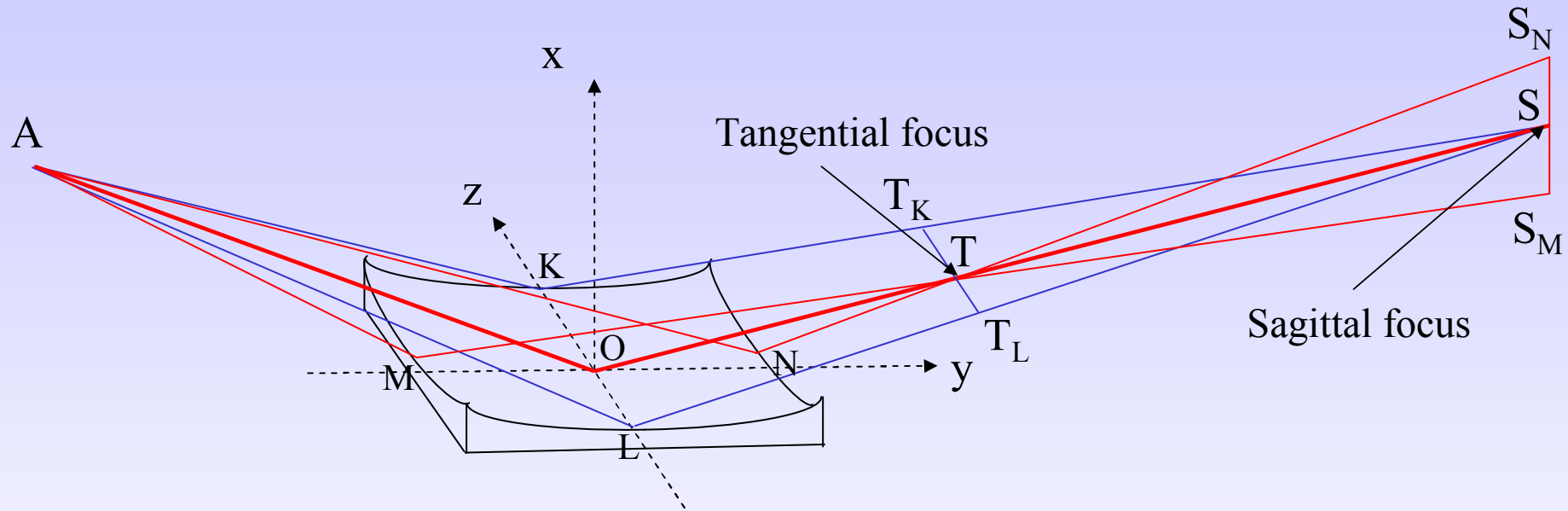
Toroid (1)



$$x^2 + y^2 + z^2 = 2Rx - 2R(R - \rho) + 2(R - \rho)\sqrt{(R - x)^2 + y^2}$$

The bicycle tyre toroid is generated rotating a circle of radius ρ in an arc of radius R .

Toroid (2)



In general, a toroid produces two non-coincident foci: one in the tangential focal plane and one in the sagittal focal plane

Tangential focus T:

$$\left(\frac{1}{r} + \frac{1}{r'_t} \right) \frac{\cos \mathcal{G}}{2} = \frac{1}{R}$$

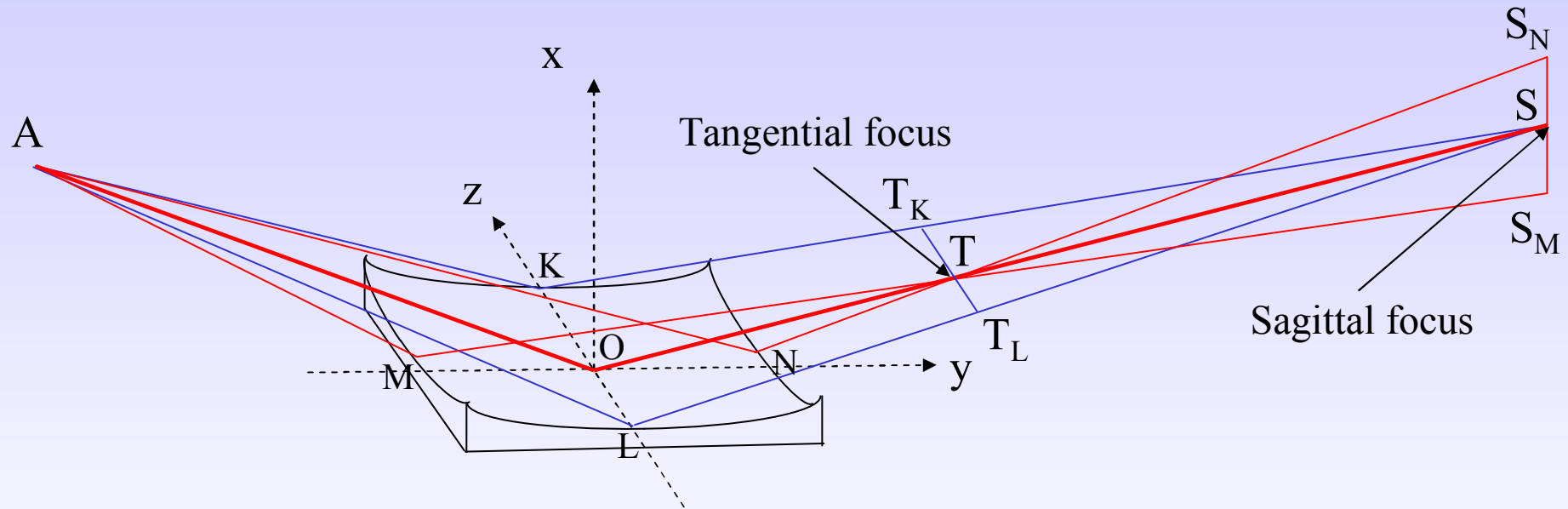
Sagittal focus S:

$$\left(\frac{1}{r} + \frac{1}{r'_s} \right) \frac{1}{2 \cos \mathcal{G}} = \frac{1}{\rho}$$

Stigmatic image:

$$\frac{\rho}{R} = \cos^2 \mathcal{G}$$

Spherical mirror

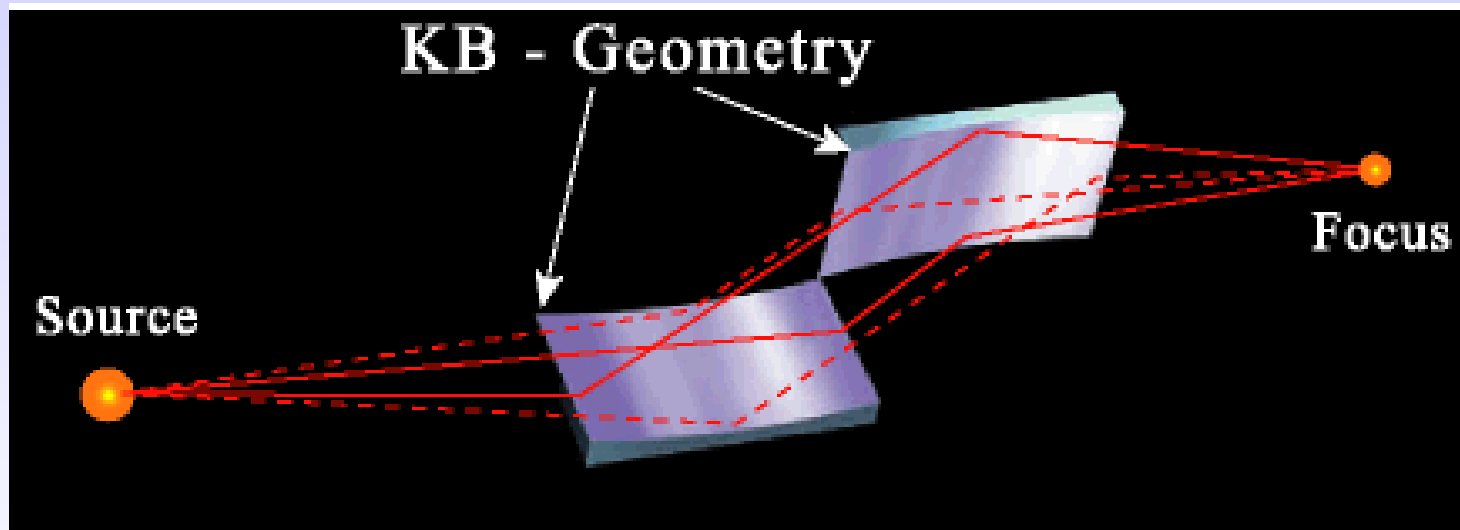


For $\rho=R \rightarrow$ **spherical mirror** :

A stigmatic image can only be obtained at normal incidence.

For a vertical deflecting spherical mirror at grazing incidence the horizontal sagittal focus is always further away from the mirror than the vertical tangential focus. The mirror only weakly focalizes in the sagittal direction.

Kirkpatrick-Baez focusing system

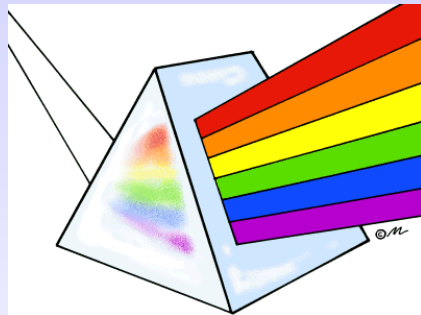


This configuration, originally suggested by Kirkpatrick and Baez in 1948, is based on two mutually perpendicular concave spherical mirrors.

Monochromators

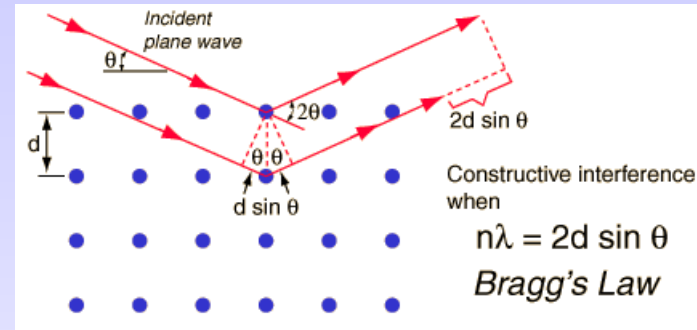
Micro wave	I.R.	Visible	U.V.	Soft X-ray	Hard X-ray
------------	------	---------	------	------------	------------

Prism

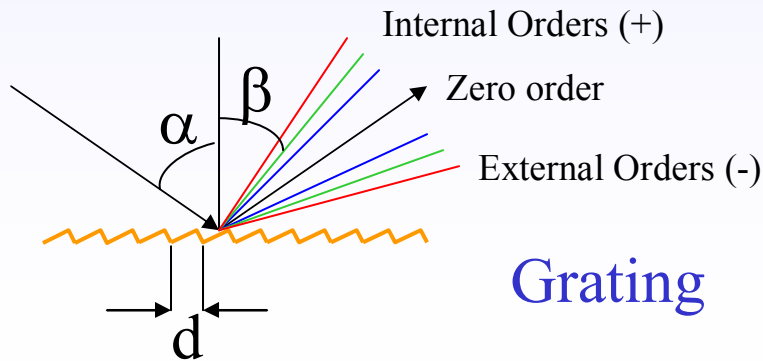


Micro wave	I.R.	Visible	U.V.	Soft X-ray	Hard X-ray
------------	------	---------	------	------------	------------

Crystal



Micro wave	I.R.	Visible	U.V.	Soft X-ray	Hard X-ray
------------	------	---------	------	------------	------------



Grating

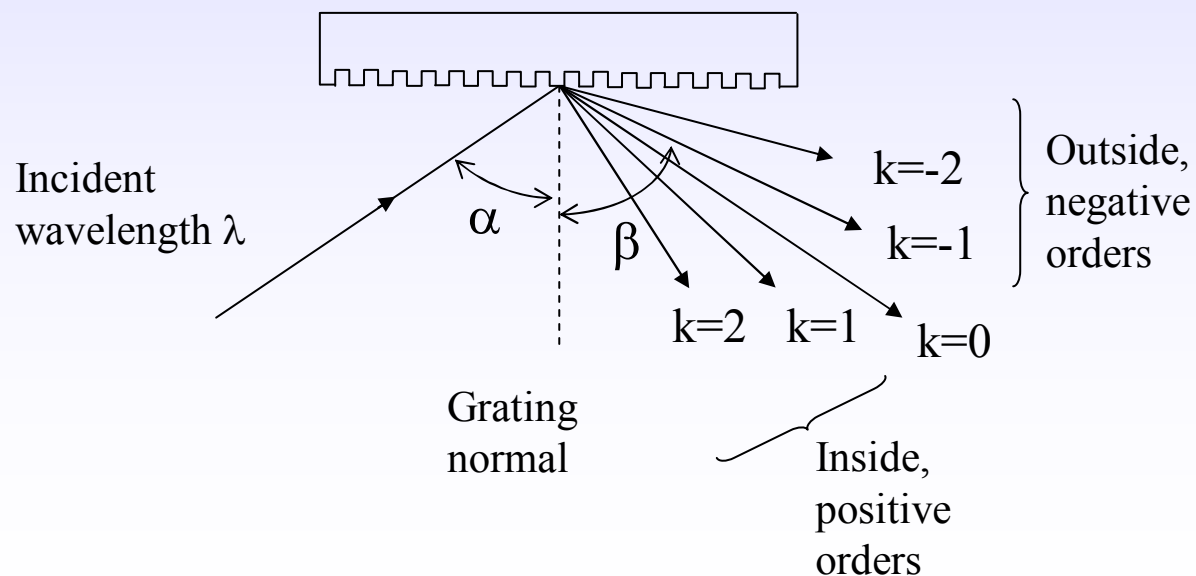
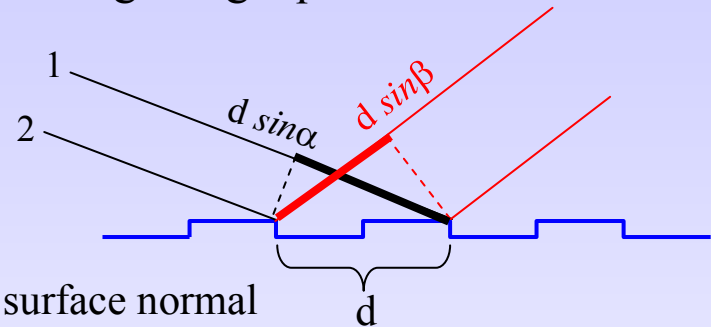


Gratings

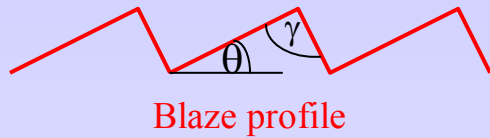
The diffraction grating is an artificial periodic structure with a well defined period d .
The diffraction conditions are given by the well-known grating equation:

$$\sin \alpha + \sin \beta = Nk\lambda$$

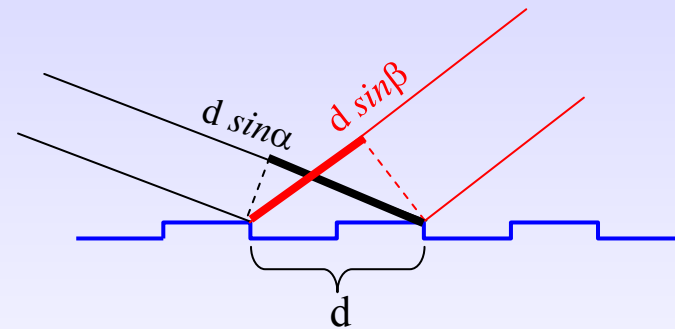
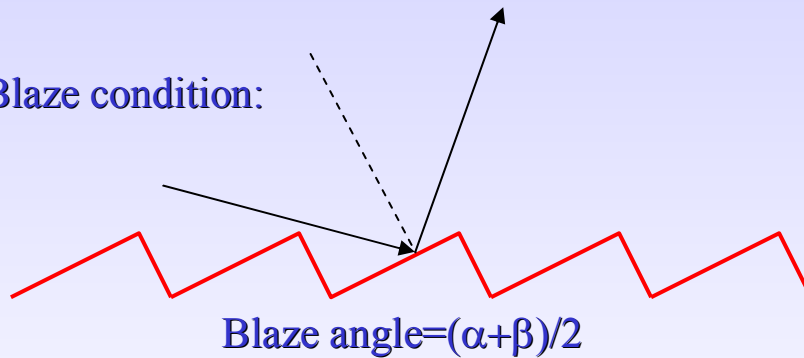
α and β are of opposite sign if on opposite sides of the surface normal
 $N=1/d$ is the groove density, k is the order of diffraction ($\pm 1, \pm 2, \dots$)



Gratings profiles (1)



Blaze condition:



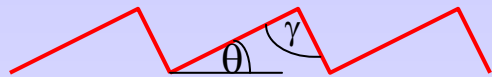
The angle θ is chosen such that for a given wavelength the diffraction direction coincides with the direction of specular reflection from the individual facets

$$k\lambda = d(\sin \alpha + \sin \beta)$$

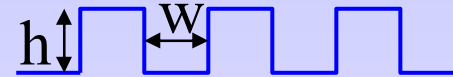
Blaze gratings: higher efficiency

Lamellar gratings: higher spectral purity

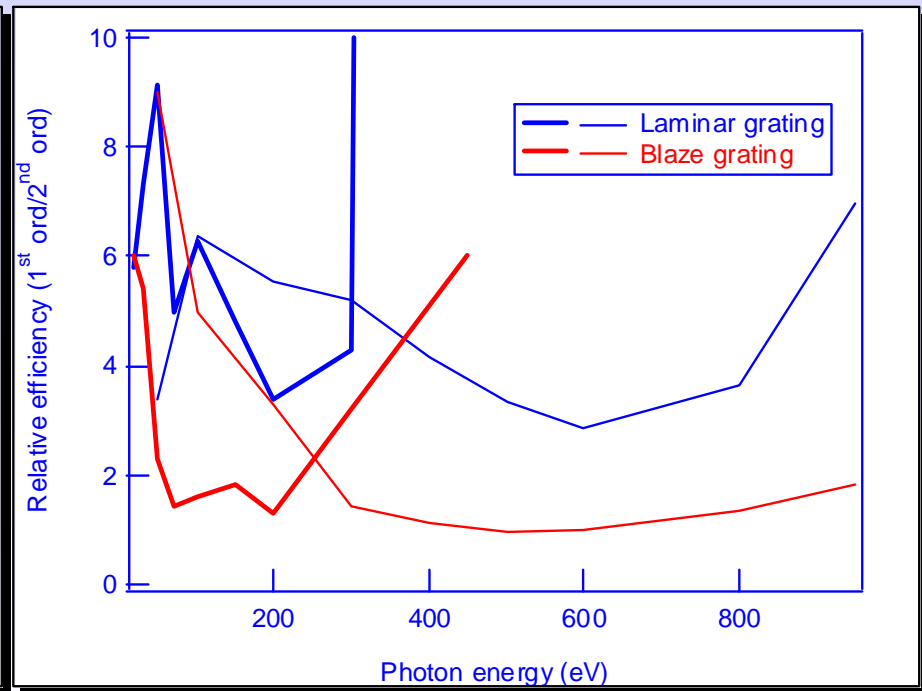
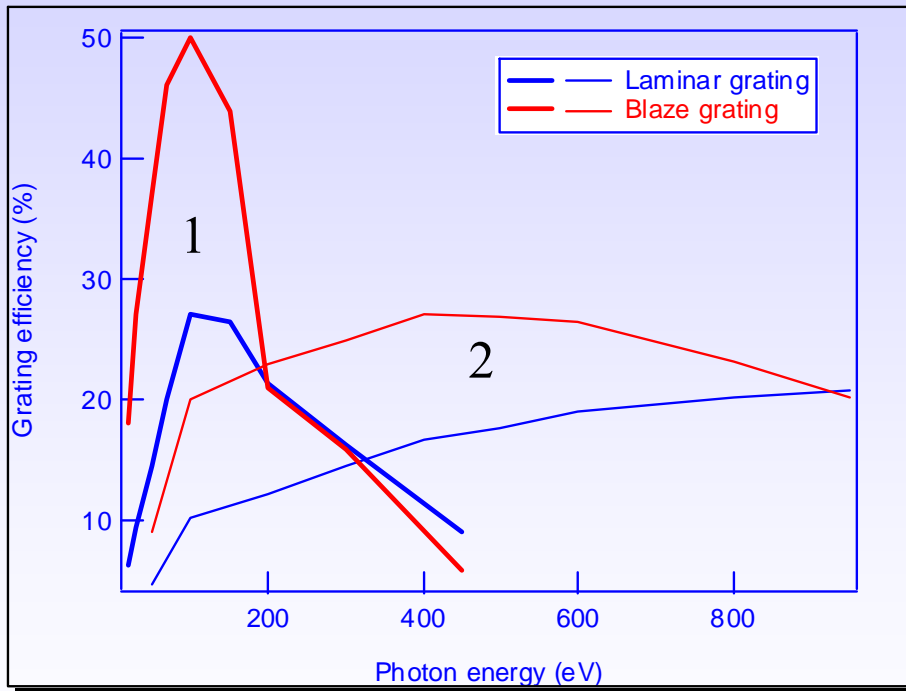
Gratings profiles (2)



Blaze profile



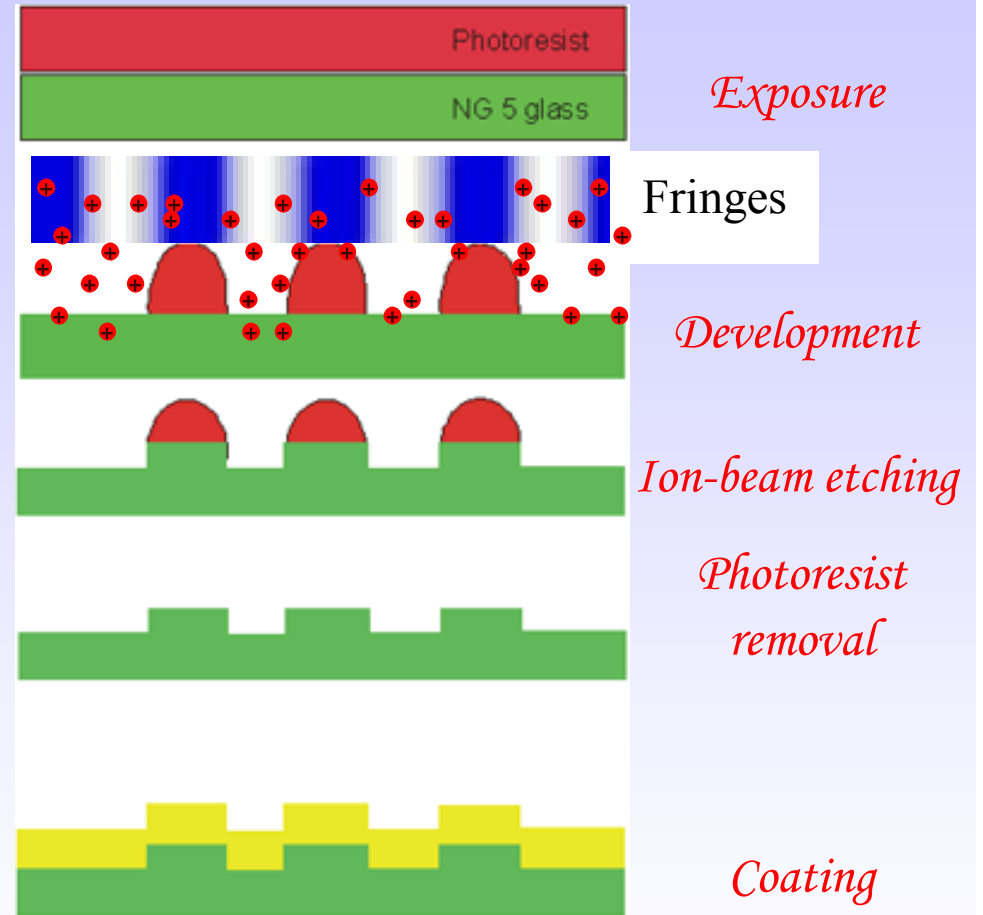
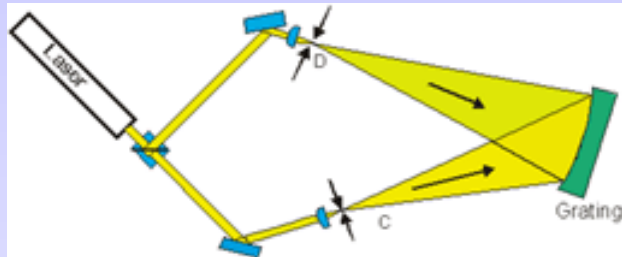
Lamellar profile



Grating 1: $N=200$ g/mm ($d=5\mu\text{m}$)
 Grating 2: $N=400$ g/mm ($d=2.5\mu\text{m}$)

$$d(\sin \alpha + \sin \beta) = k\lambda$$

Holographically recorded grating



Grating resolving power (1)

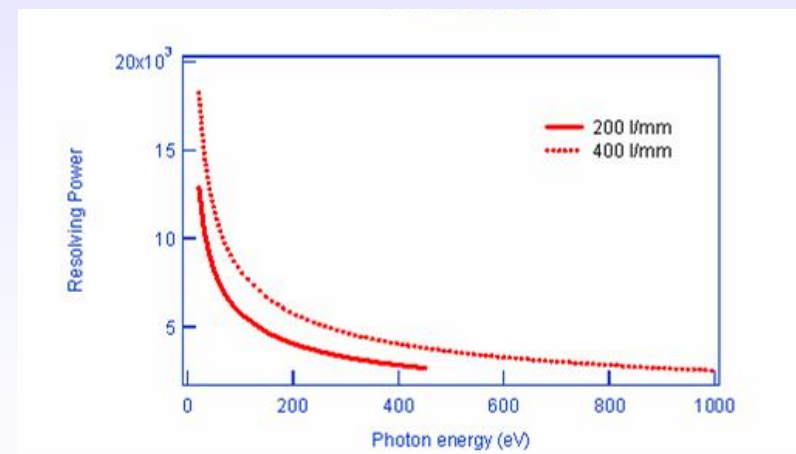
Differentiating the grating equation: $\sin \alpha + \sin \beta = Nk\lambda$
the **angular dispersion** of the grating is obtained:

(higher groove density \rightarrow higher angular dispersion)

$$\Delta\lambda = \frac{\cos \beta}{Nk} \Delta\beta$$

The **resolving power** is defined as:

$$R = \frac{E}{\Delta E} = \frac{\lambda}{\Delta\lambda}$$



$$R=10000 \text{ @}100\text{eV} \rightarrow \Delta E=100\text{eV}/10000=10\text{meV}$$

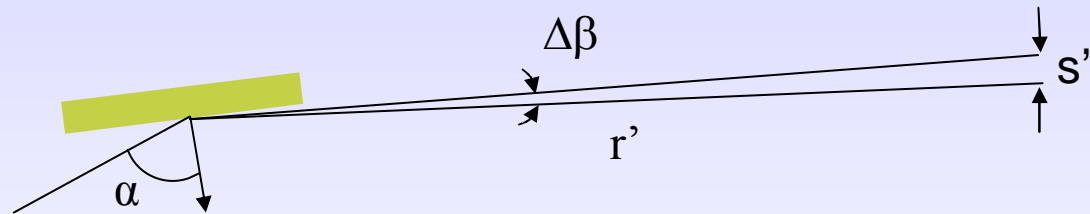
Grating resolving power (2)

Angular dispersion : $\Delta\lambda = \frac{\cos \beta}{Nk} \Delta\beta$

Resolving power: $R = \frac{E}{\Delta E} = \frac{\lambda}{\Delta\lambda}$

The main contribution is from the width s' of the exit slit:

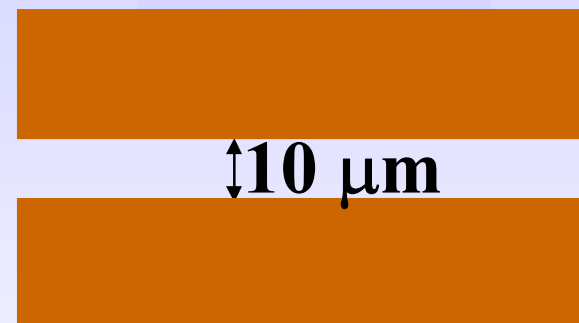
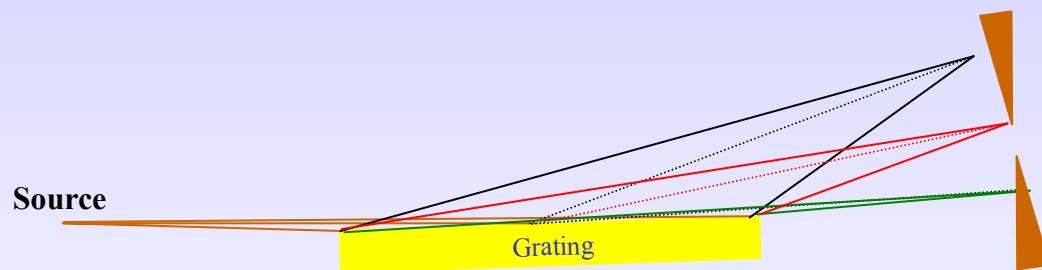
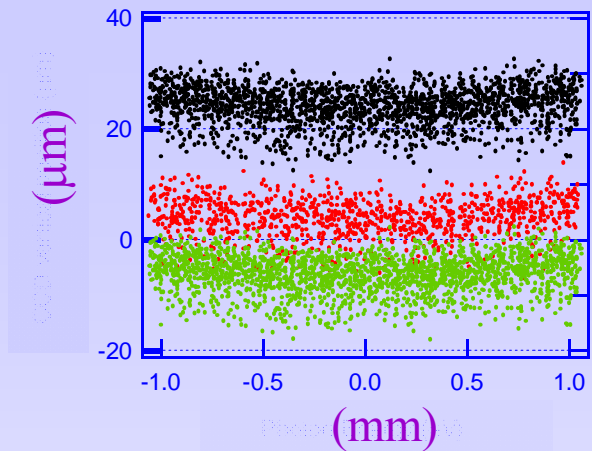
$$\frac{E}{\Delta E} = \frac{\lambda}{\Delta\lambda} = \frac{\lambda N k r'}{(\cos \beta) s'}$$



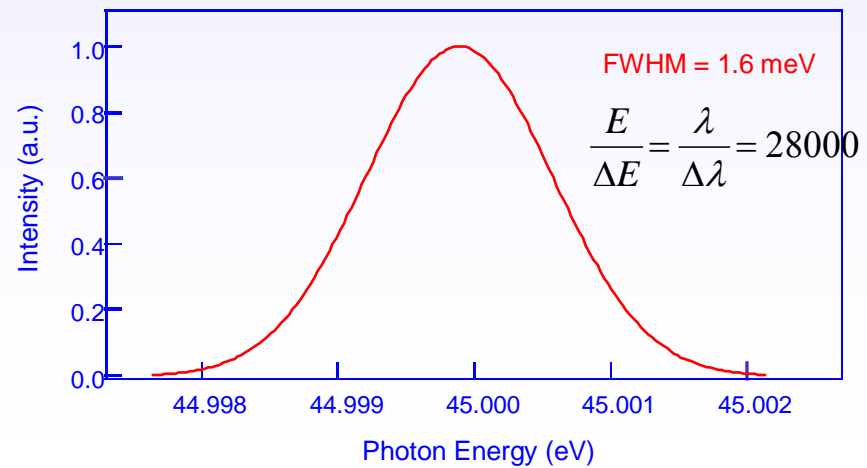
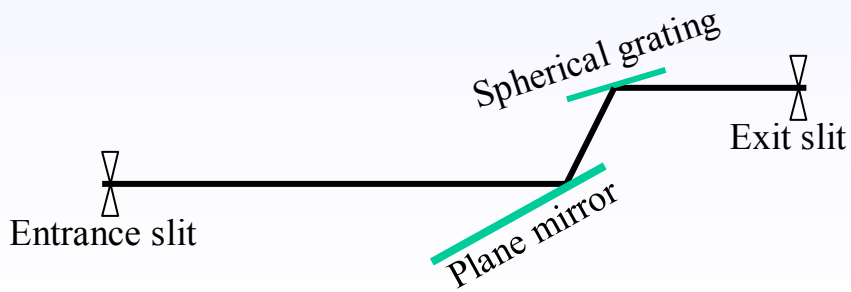
The entrance slit contribution is similar:

$$\frac{E}{\Delta E} = \frac{\lambda}{\Delta\lambda} = \frac{\lambda N k r}{(\cos a) s}$$

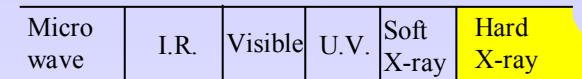
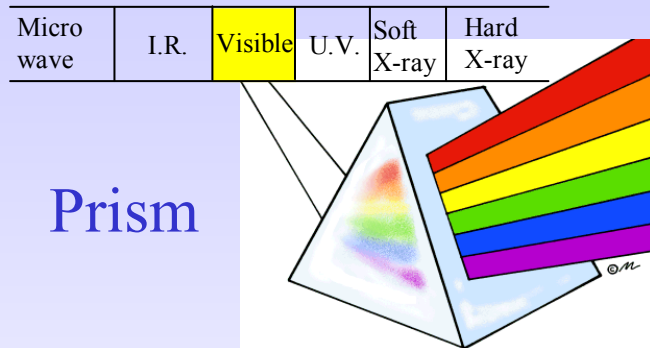
Grating resolving power (3)



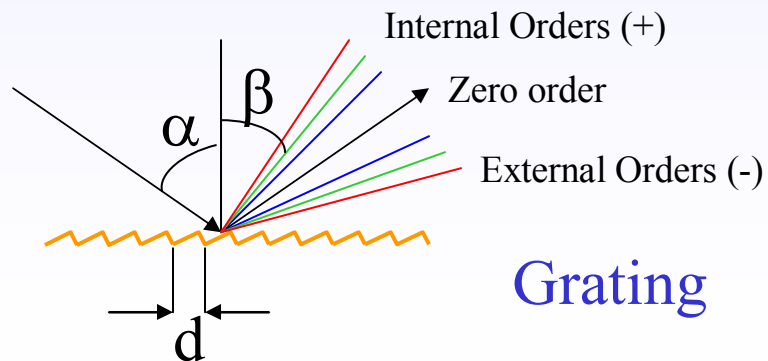
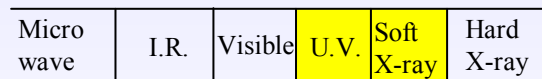
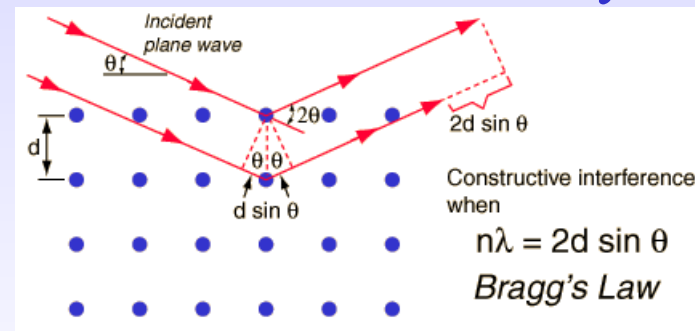
Exit slit



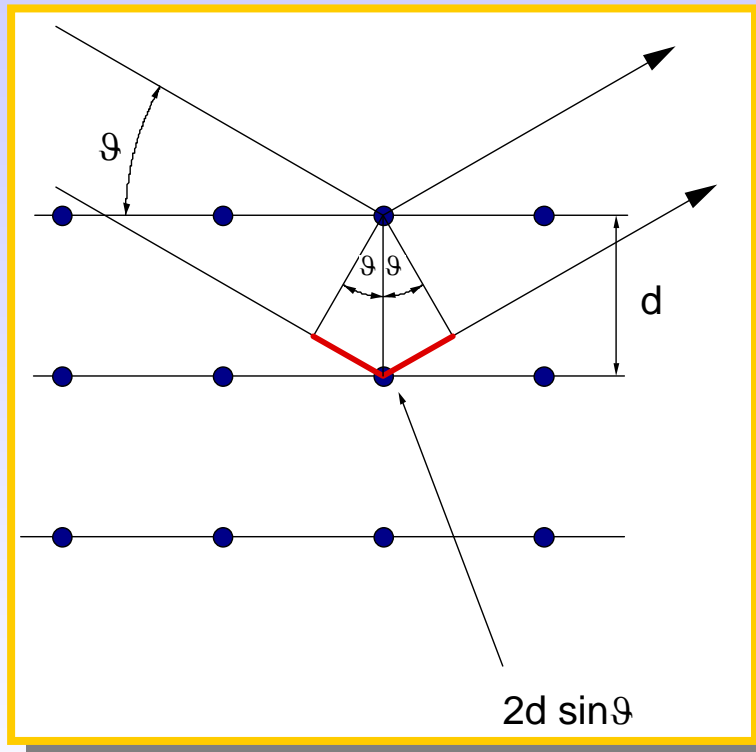
Monochromators



Crystal



Bragg's law



Radiation of wavelength λ is reflected by the lattice planes. The outgoing waves interfere. The interference is constructive when the optical path difference is a multiple of λ :

$$2d \sin \theta = n \lambda$$

d is the distance between crystal planes.

$$\sin \theta \leq 1 \Rightarrow \lambda \leq \lambda_{\max} = 2d$$

The maximum reflected wavelength corresponds to the case of normal incidence: $\theta = 90^\circ$

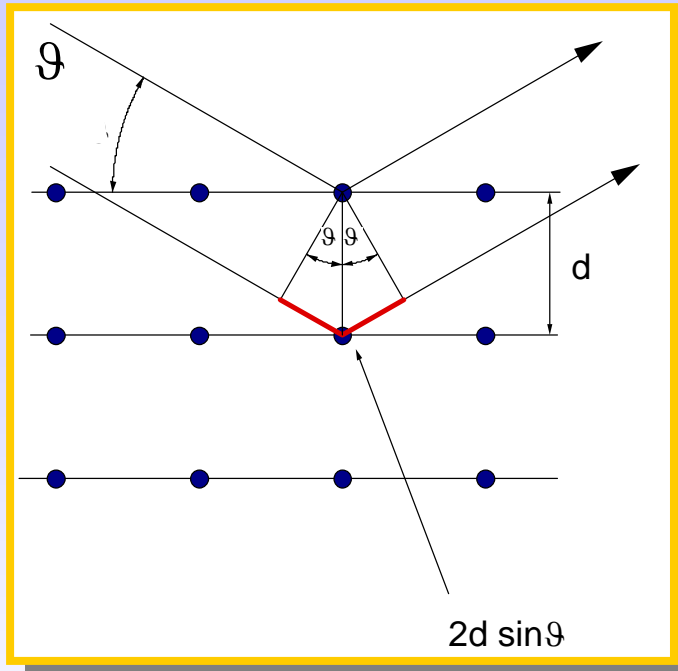
EXAMPLES: $Si(111): d = 3.13 \text{ \AA} \rightarrow E_{\min} \approx 2 \text{ keV}$

$Si(311): d = 1.64 \text{ \AA} \rightarrow E_{\min} \approx 3.8 \text{ keV}$

$InSb(111): d = 3.74 \text{ \AA} \rightarrow E_{\min} \approx 1.7 \text{ keV}$

$Be(10\bar{1}0): d = 7.98 \text{ \AA} \rightarrow E_{\min} \approx 0.8 \text{ keV}$

Energy resolution



$$\frac{\Delta \lambda}{\lambda} = \frac{\Delta E}{E} = \Delta \mathcal{G} \frac{\cos \mathcal{G}}{\sin \mathcal{G}}$$

The energy resolution of a crystal monochromator is determined by the angular spread $\Delta \mathcal{G}$ of the diffracted beam and by the Bragg angle \mathcal{G}

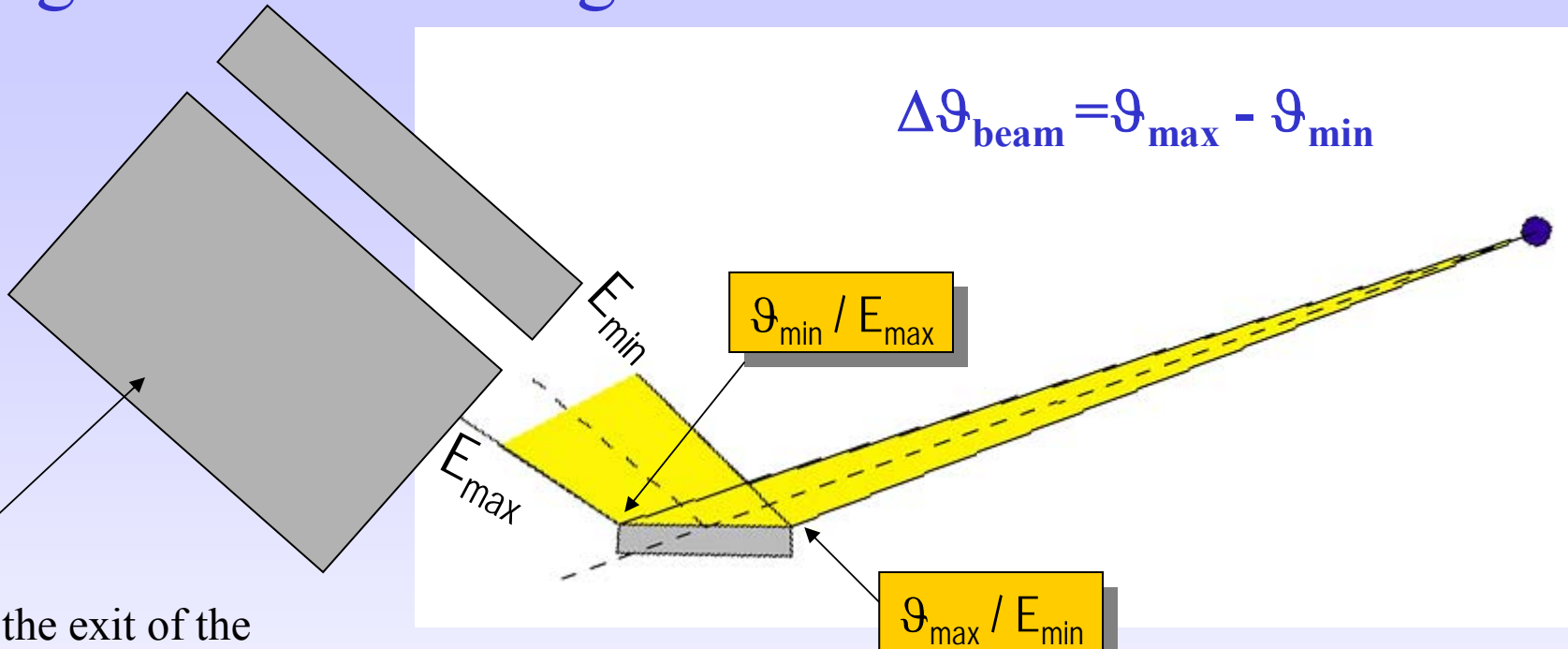
$\Delta \mathcal{G}$ has two contributions :

$\Delta \mathcal{G}_{\text{beam}}$: angular divergence of the incident beam

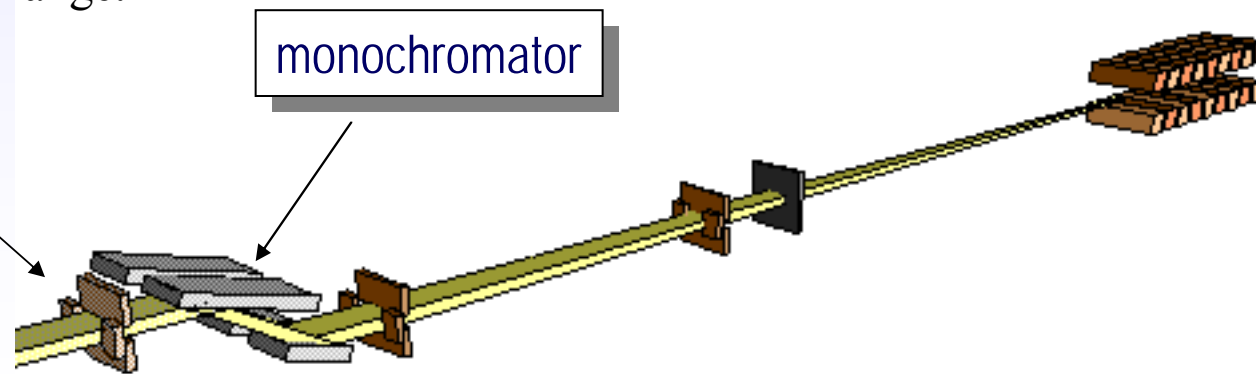
ω_{crystal} : intrinsic width of the Bragg reflection

Angular beam divergence

$$\Delta\vartheta_{\text{beam}} = \vartheta_{\text{max}} - \vartheta_{\text{min}}$$

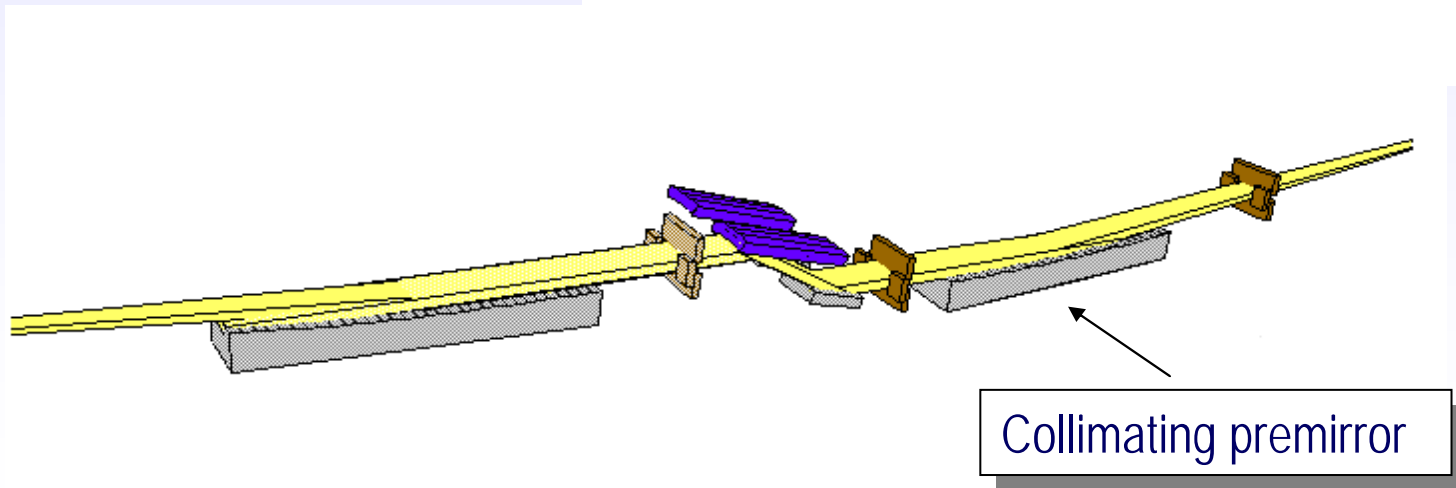
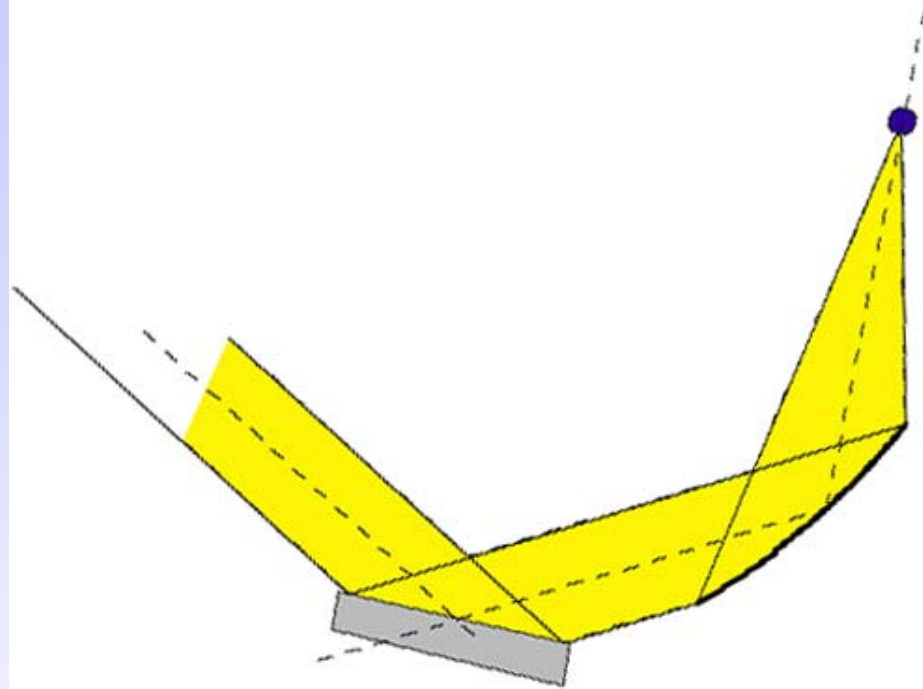


A slit at the exit of the monochromator selects a narrower energy range.



Collimating mirror

A collimating mirror in front of the crystal reduces the angular divergence $\Delta\theta_{\text{beam}}$ of the incident beam, improving the energy resolution.

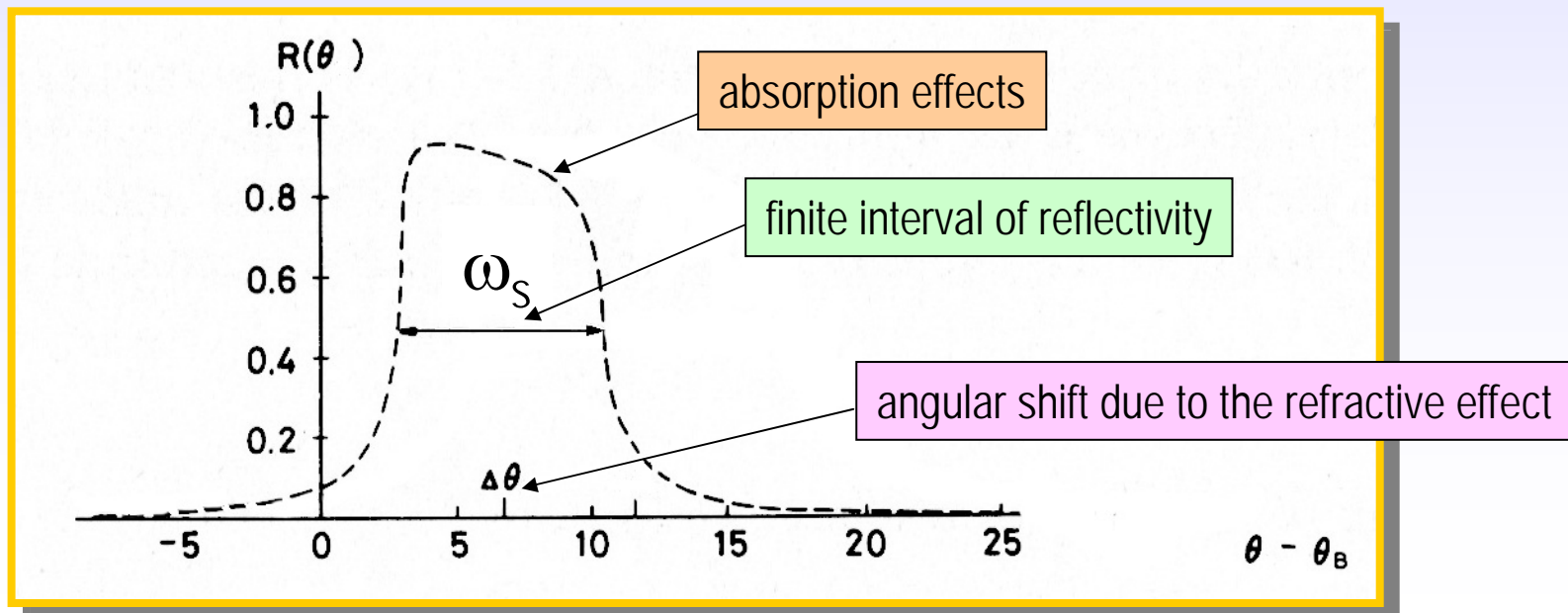


Darwin Curve

The intrinsic reflection width of the crystal, ω_S , can be obtained measuring the crystal reflectivity for a perfectly collimated monochromatic beam, as a function of the difference between the actual value of the incidence θ angle and the ideal Bragg value: $\Delta\theta = \theta - \theta_B$.

This reflectivity is derived by the dynamic diffraction theory, which includes multiple scattering \rightarrow **Darwin curve**:

1. there is a finite interval of incident angles for which the beam is reflected
2. the center of this interval does not coincide with the Bragg angle
3. $R < 1$ and has a typical asymmetric shape

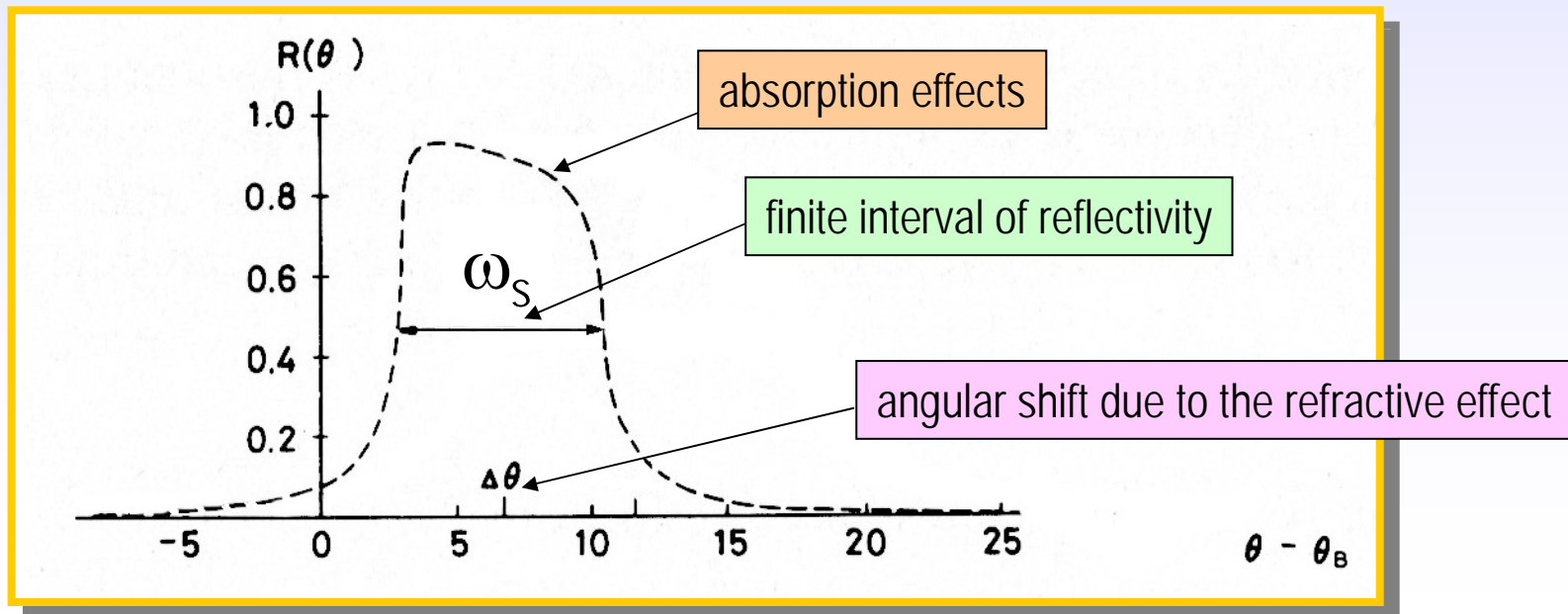


Intrinsic width of the Bragg reflection

$$\omega_S = \frac{2 r_e \lambda^2}{\sin(2\vartheta_B) \pi V} C |F_{hr}| e^{-M}$$

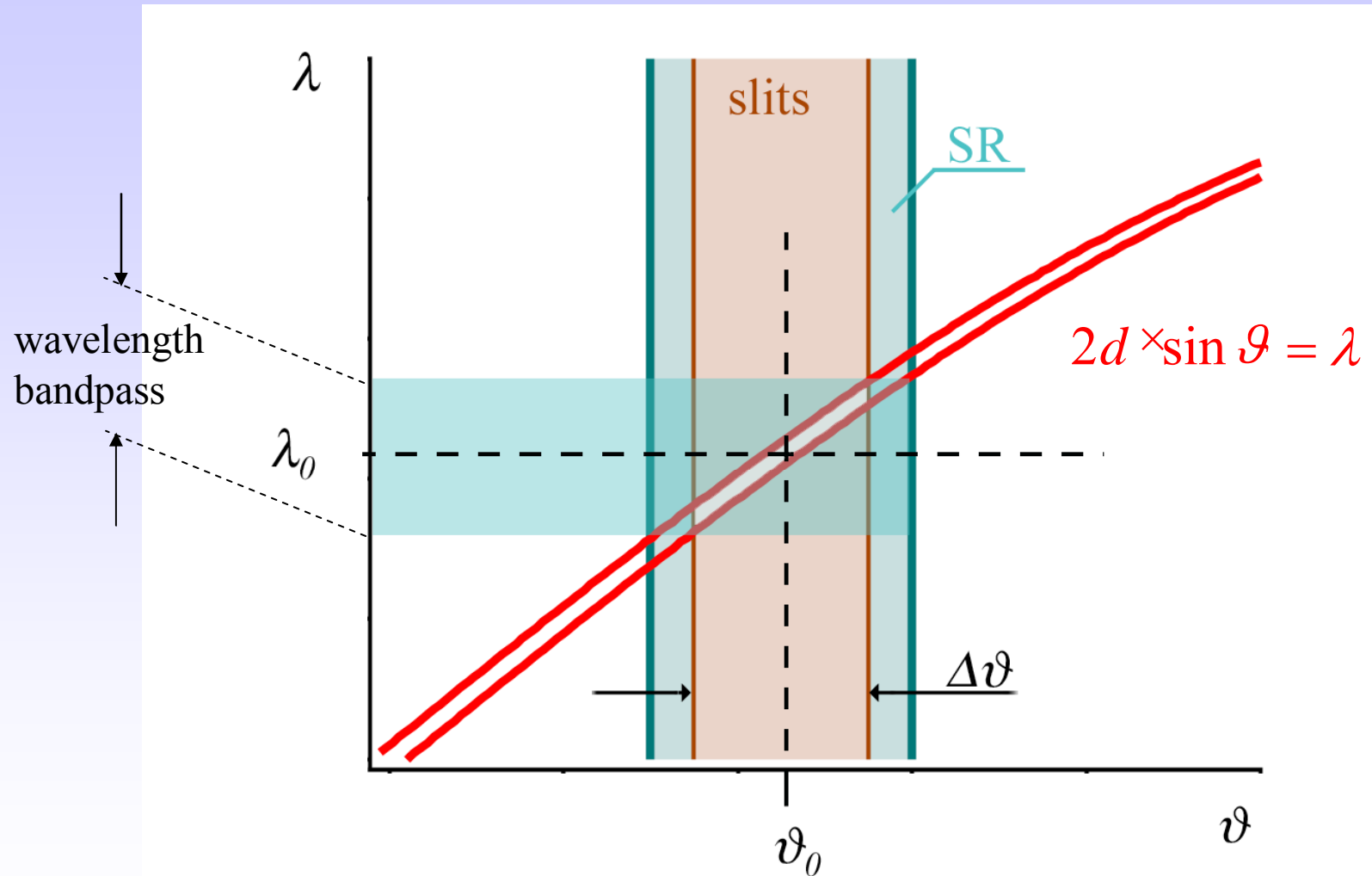
Dynamic diffraction theory

θ_B	Bragg angle
λ	wavelength of radiation
r_e	radius of the electron e^2/mc^2
V	volume of the unit cell
C	polarization factor
$ F_{hr} $	amplitude of the crystal structure factor F_r , related to the (hkl) diffraction
e^{-M}	temperature factor



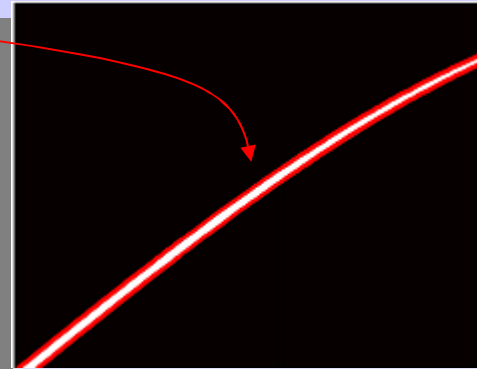
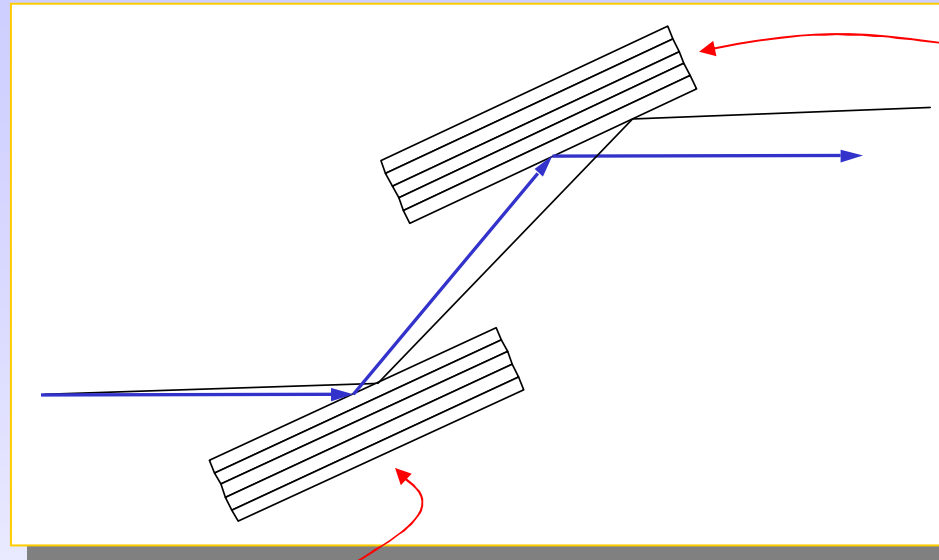
Du Mond diagram

$\Delta\vartheta =$ angular acceptance of the slit

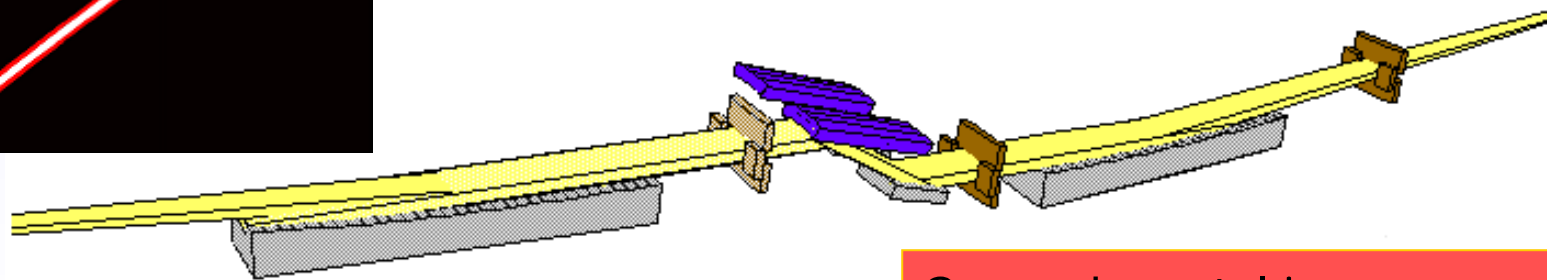
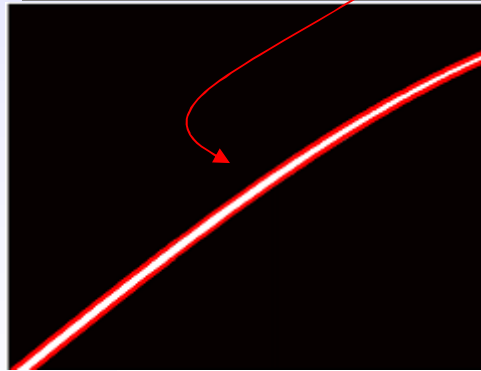


The Du Mond diagram describes the reflection of radiation by the crystal in the $\vartheta - \lambda$ space.

Crystal Monochromators

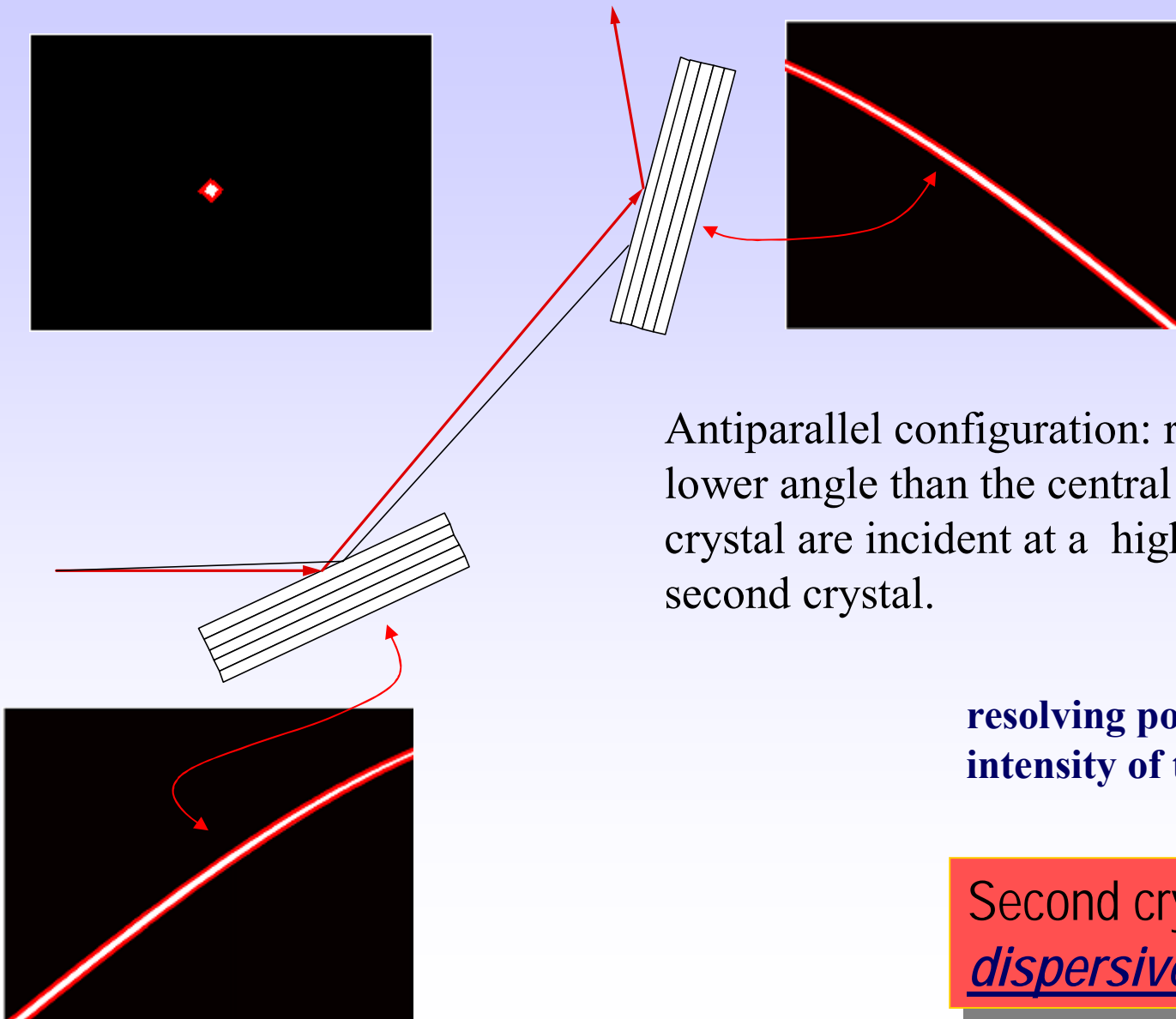


Parallel geometry:
all rays accepted by the first
crystal are accepted also by the
second.



Second crystal in
non dispersive configuration

Crystal Monochromators

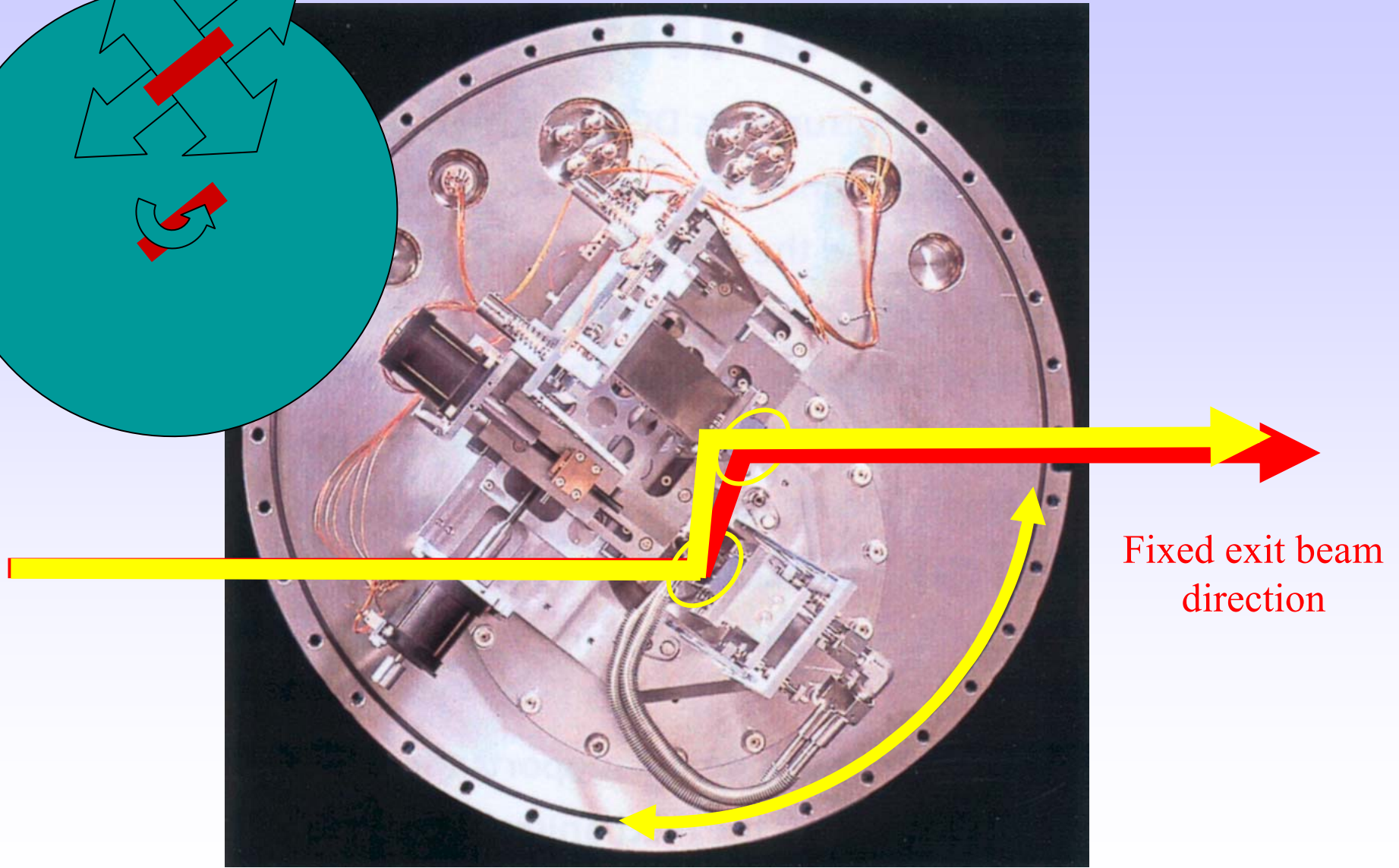
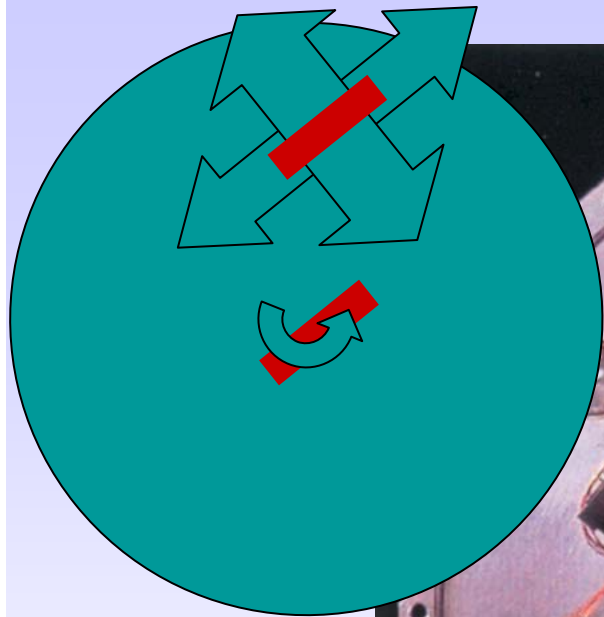


Antiparallel configuration: rays incident at a lower angle than the central ray on the first crystal are incident at a higher angle on the second crystal.

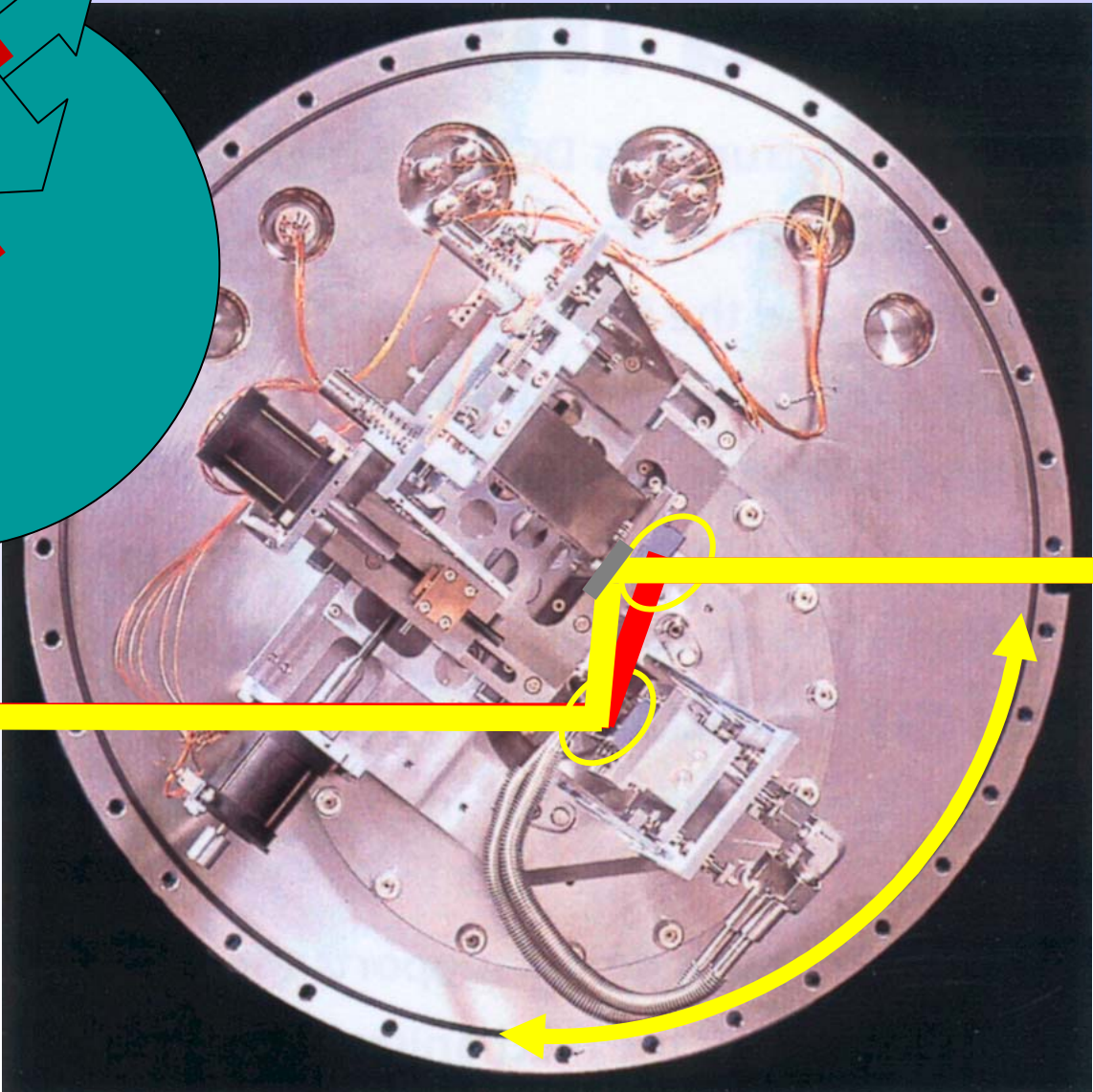
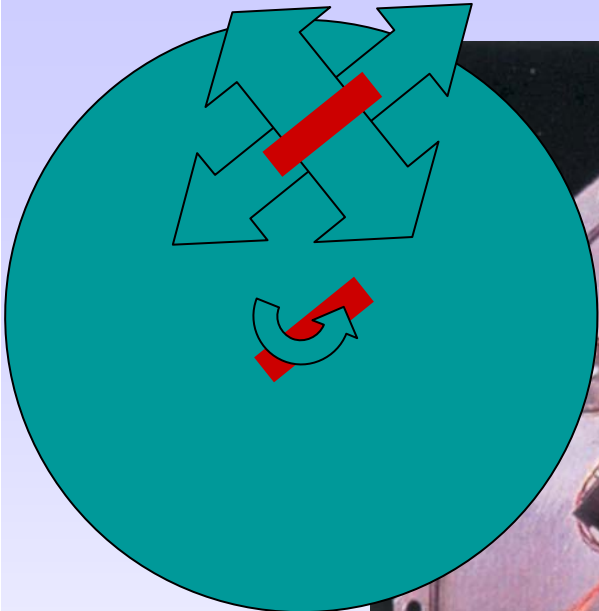
resolving power \uparrow
intensity of the reflection \downarrow

Second crystal in dispersive configuration

Double Crystal Monochromator

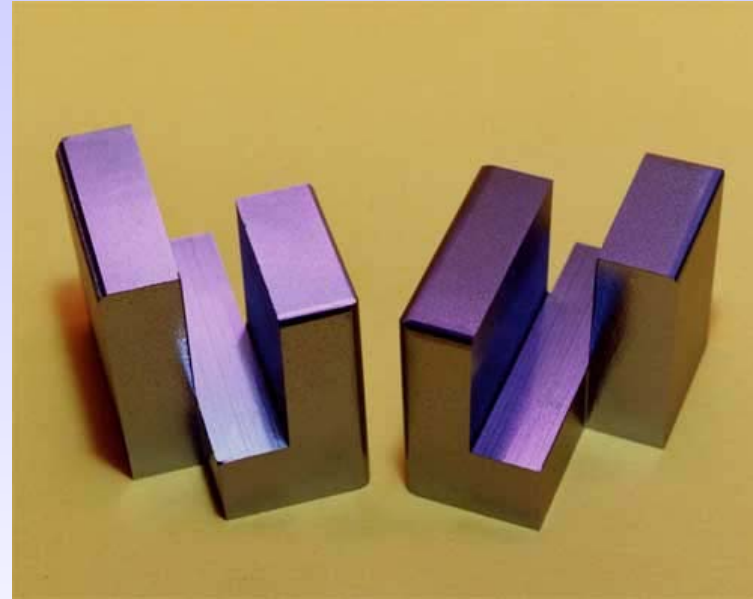


Double Crystal Monochromator

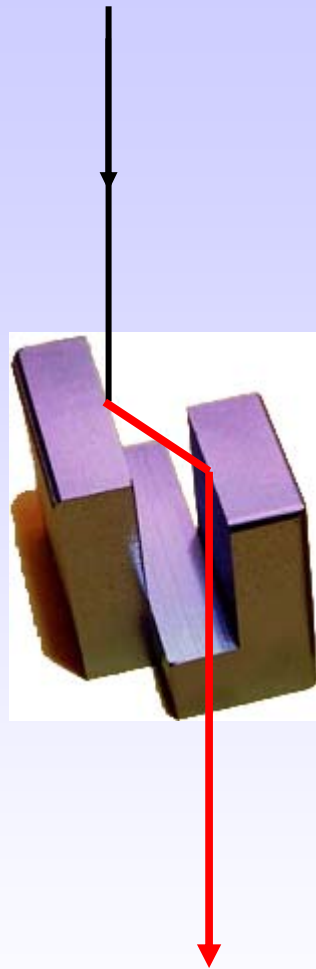


Fixed exit beam direction

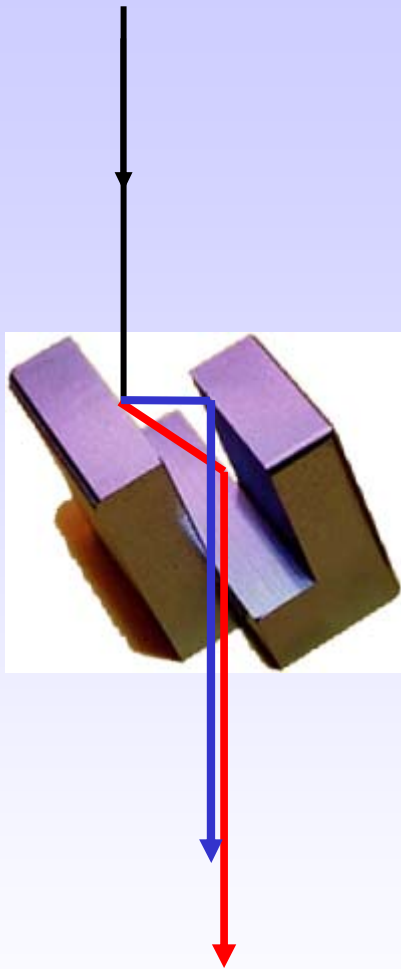
Channel-cut



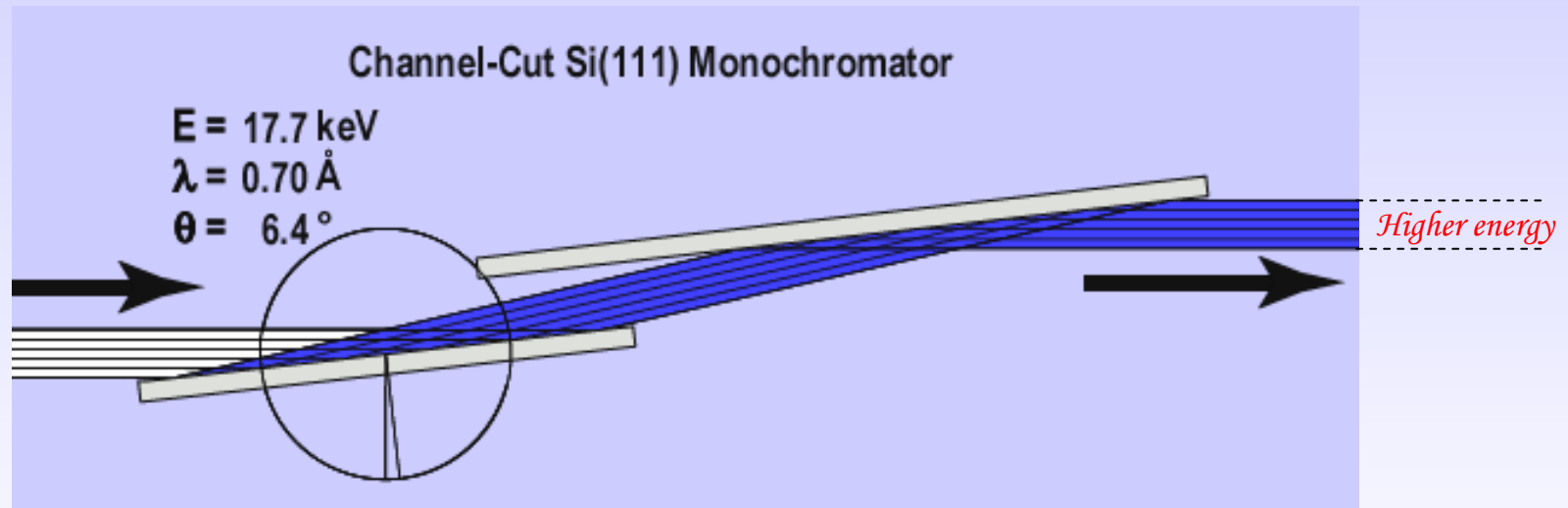
Channel-cut



Channel-cut

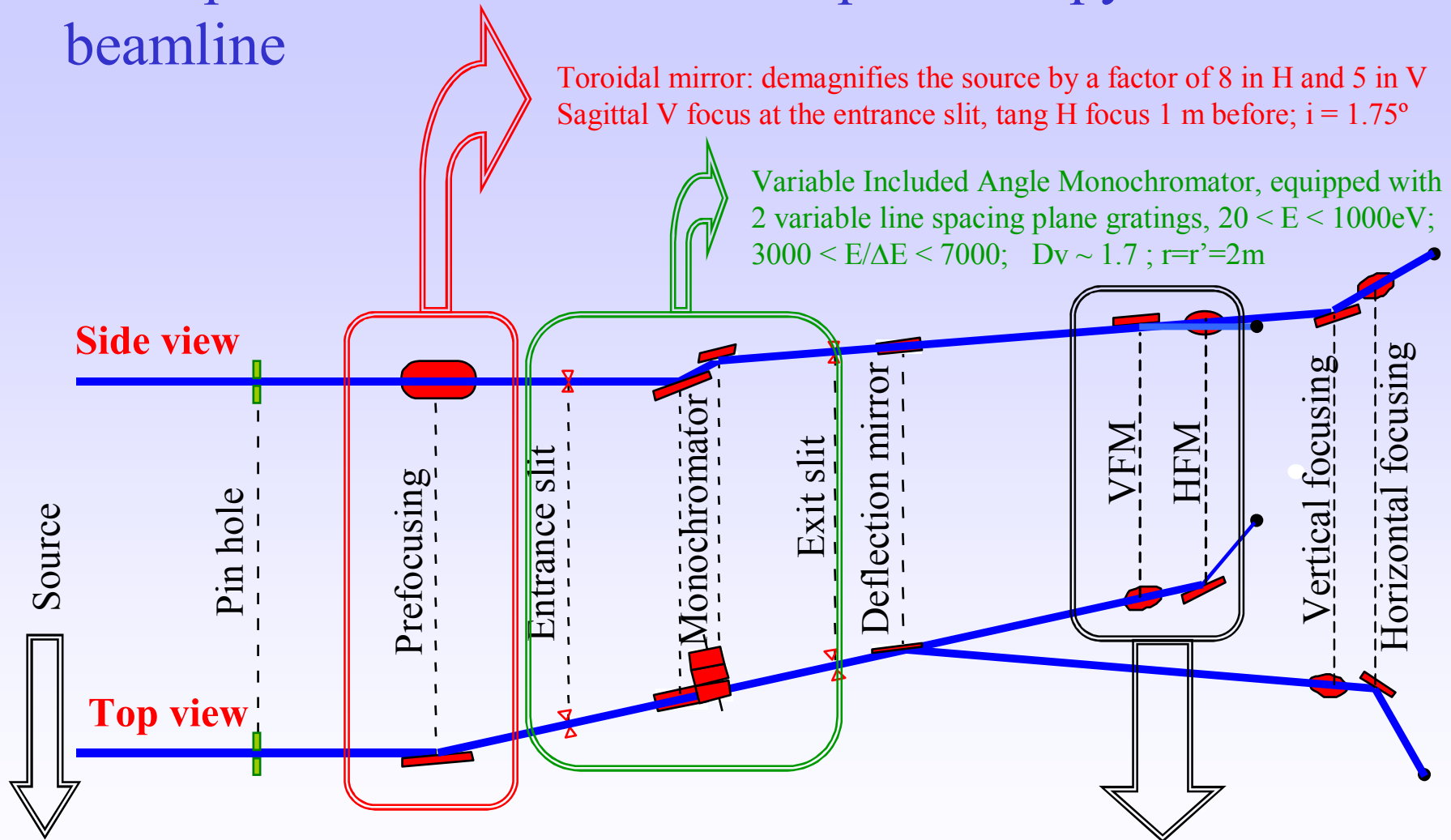


Channel-cut



Much easy to align
Exit beam displacement

Example: the ELETTRA Nanospectroscopy beamline



two APPLE-II helical undulators,
Photon energy: 20 - 1000eV
Size @400eV: $560\mu\text{m} \times 50\mu\text{m}$;
 $110\mu\text{rad} \times 85\mu\text{rad}$ (FWHM)

Two bendable elliptical cylinder mirrors, in KB geometry:
demagnification factors are 10 in H and 5 in V, $i = 2^\circ$
About 1×10^{12} photons/s are focused in a $7\mu\text{m} \times 2\mu\text{m}$ spot.

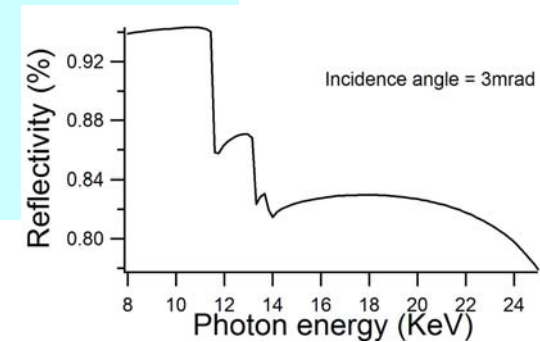
Example: the ELETTRA X-ray Diffraction beamline

Experiment

Source distance = 41.5m
 Energy range: 4-21KeV
 spot size: 0.4x0.2mm²
 Photon flux: 10¹²ph/s (at $\lambda=1\text{\AA}$)
 Energy resolution: 3-4000

Cylindrical mirror for vertical collimation

Silicon with 50nm Platinum coating
 Mirror length=1.4m
 $i=3\text{mrad}$; Vertical angular acceptance = 180 μrad
 Radius=14Km
 Source distance $d=22\text{m}$
 Collimated beam vertical divergence <10 μrad

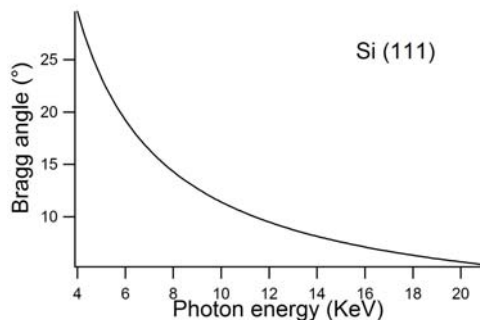


Toroidal focusing mirror

Sagittal cylindrical bendable mirror
 Tangential radius = 9Km
 (variable: 5Km - ∞)
 Sagittal radius = 5.5cm
 Source distance = 28m
 H demagnification = 2
 V demagnification = 1.6

Double crystal monochromator

Si(111) flat crystals, in non-dispersing configuration
 $\omega_s = 7.4^\circ = 35\mu\text{rad}$ @8KeV
 Source distance=24m
 250W absorbed by the 1 $^\circ$ crystal

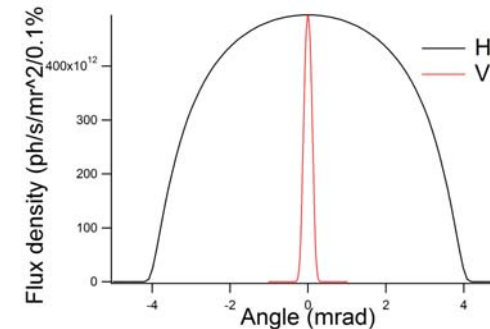


Pyrolytic graphite filters to absorb $E < 4.2\text{KeV}$

Slits, H angular acceptance: 1.5mrad

Multi-pole wiggler

57 poles, 1.5T magnetic field,
 14cm period length,
 5.8KeV critical energy @2.4GeV
 5 kW total power @140mA



References (1)

These notes have been taken from:

- D.Attwood, “Soft x-rays and extreme ultraviolet radiation”, Cambridge University Press, 1999
- B.W.Batterman and D.H.Bilderback, “X-Ray Monochromators and Mirrors” in “Handbook on Synchrotron Radiation”, Vol.3, G.S.Brown and D.E.Moncton, Editors, North Holland, 1991, chapter 4
- “Selected Papers on VUV Synchrotron Radiation Instrumentation: Beam Line and Instrument Development”, D.L.Ederer Editor, SPIE vol. MS 152, 1998
- W.Gudat and C.Kunz, “Instrumentation for Spectroscopy and Other Applications”, in “Synchrotron Radiation”, “Topics in Current Physics”, Vol.10, C.Kunz, Editor, Springer-Verlag, 1979, chapter 3
- M.Howells, “Gratings and monochromators”, Section 4.3 in “X-Ray Data Booklet”, Lawrence Berkeley National Laboratory, Berkeley, 2001
- M.C. Hutley, “Diffraction Gratings”, Academic Press, 1982

References (2)

- R.L. Johnson, “Grating Monochromators and Optics for the VUV and Soft-X-Ray Region” in “Handbook on Synchrotron Radiation”, Vol.1, E.E.Koch, Editor, North Holland, 1983, chapter 3
- G.Margaritondo, “Introduction to Synchrotron Radiation”, Oxford University Press, 1988
- T.Matsushita, H.Hashizume, “X-ray Monochromators”, in “Handbook on Synchrotron Radiation”, Vol.1b, E.-E. Koch, Editor, North Holland, 1983, chapter 4
- W.B.Peatman, “Gratings, mirrors and slits”, Gordon and Breach Science Publishers, 1997
- J.Samson and D.Ederer, “Vacuum Ultraviolet Spectroscopy I and II”, Academic Press, San Diego, 1998
- J.B. West and H.A. Padmore, “Optical Engineering” in “Handbook on Synchrotron Radiation”, Vol.2, G.V.Marr, Editor, North Holland, 1987, chapter 2
- G.P.Williams, “Monocromator Systems”, in “Synchrotron Radiation Research: Advances in Surface and Interface Science”, Vol.2, R.Z.Bachrach, Editor, Plenum Press, 1992, chapter 9

Programs

- **Shadow**
(ray tracing) http://www.nanotech.wisc.edu/CNT_LABS/shadow.html
- **XOP**
(general optical calculations) <http://www.esrf.eu/computing/scientific/xop2.1/intro.html>
- **SPECTRA**
(optical properties of synchrotron radiation emitted from bending magnets, wigglers and undulators) http://radiant.harima.riken.go.jp/spectra/index_e.html

Useful link: <http://www-cxro.lbl.gov/index.php?content=/tools.html>